Mechanisms of antiepileptic drug action underlying neural tube defects

By

KAYLA HORTON SPARKS

DISSERTATION

Submitted in partial satisfaction of the requirements for the degree of

DOCTOR OF PHILOSOPHY

in

Pharmacology and Toxicology

in the

OFFICE OF GRADUATE STUDIES

of the

UNIVERSITY OF CALIFORNIA

DAVIS

Approved:

Laura N. Borodinsky, Chair

David Pleasure

Angela Gelli

Committee in Charge

2022

ACKNOWLEDGMENTS

It takes a village. I would like to acknowledge the many people that have supported me and made this work possible.

To my mentor Dr. Laura Borodinsky; I truly would not be at this milestone without you. Thank you for providing an environment in which I could grow my love for science. You have been an incredible support of my professional and scientific goals while honoring my role as a mother. Thank you for cheering me on and reminding me that I am capable of building my family while chasing my dreams. The kindness that you have shown me is something that I will continue to cherish. This pandemic has brought unprecedented stressors that you have navigated beautifully, remaining a constant source of support and empathy to your students. Thank you for allowing me the independence to mature as a scientist and develop my project, while providing unique perspective and insight. You have advance ed my skills in experimental design, critical thinking, data analysis, and scientific communication. You are brilliant with a heart of gold and I feel fortunate to have had the opportunity to learn from you.

To the Borodinsky lab; Thank you for welcoming me with open arms and helping me get this project off the ground. A special thank you to Olesya Visina for all of your administrative help and training, as well as facilitating the success of these experiments during the challenging times brought on by the pandemic. Raman Goyal for the beautiful work that laid the foundation for this thesis and for your support as a fellow mother and scientist. Andrew Hamilton for always knowing how to make me laugh and helping me brainstorm when I hit a wall. Olga (the Western Blot Warrior) Balashova for your expertise and patience in helping me troubleshoot and advance the scope of this work.

To my advisor Dr. Heather Knych; Thank you for providing me a safe place to find clarity and for encouraging me to persevere through tough times. You are an incredible scientist and mentor that I feel fortunate to have had alongside me on this journey.

To my parents; Since I was a little girl you have nurtured my curiosity, built my confidence and encouraged me to chase my dreams. You made learning fun and exciting. You practiced a healthy, balanced lifestyle consisting of personal and professional growth with family values being of upmost importance. You taught me that I could have it all – dreams of a career and a family. I truly wouldn't be the scientist or the mother that I am without the two of you. Thank you for helping me raise my babies so that I could dedicate myself to this work with the calm knowing that they were in your hands. You facilitated my transition into motherhood by seamlessly caring for Finley and Leo so that I could continue to work towards this milestone, and for that I am forever grateful.

To my siblings and best friend; Holli, thank you for always knowing what I need before I even have the chance to acknowledge or voice it. Katie, thank you for helping me transition into motherhood and for always being one call away to help me navigate the world of a working mama. Tori, thank you for the countless hours of editing my words on paper and the words between my ears. Ben, for inspiring me through your insatiable desire to live an extraordinary life and overcoming any obstacle along the way.

To my husband; Thank you for unconditionally supporting my dreams. You have been the best partner on this journey and this work would not have been possible without your love, sacrifice and dedication to our family. Thank you for helping me navigate the tough times and celebrate the accomplishments. Thank you for taking on the financial burden of raising a family with a wife in graduate school, I am grateful beyond measure for the life you provide for us. Thank you for going

above and beyond to make me feel safe, loved, appreciated and respected. This milestone is as much yours as it is mine.

To Finley and Leo; We have done this together. Thank you for being patient with mommy and sacrificing time together to make this work happen. My love for you has fueled me on this journey. You have made me stronger, better and more fulfilled than I could have ever imagined. This is for you.

ABSTRACT

Revealing the regulatory mechanisms that coordinate neural plate folding and neural tube closure could improve preventative measures for neural tube defects (NTDs). Among the most prevalent and serious birth defects, NTDs occur in 1 in 1000 births in the United States. Multiple causes, both genetic and environmental, have been recognized, including the use of antiepileptic drugs (AEDs) during pregnancy. There is a 10- to 20-fold increase in NTD incidence associated with the use of AEDs during pregnancy, but the teratogenic mechanisms are unknown. The prevalent paradigm that neural activity is not evident at early stages of development suggests that AED teratogenic effects are due to off-target mechanisms. However, recent evidence of embryonic excitability during neural tube formation has challenged this theory and supports the essential need to investigate the presence and regulation of neural activity during nervous system development.

Voltage-gated sodium channels (Na_v) are one of the most common and efficacious cellular target of AEDs in the mature nervous system yet remain relatively unexplored during neural tube formation. My findings demonstrate that Na_v are expressed by *Xenopus laevis* neural plate cells throughout neural plate folding and neural tube closure and its insertion in neural plate cell membranes increases with the progression of neural tube formation, suggesting that Na_v may play an important role in this process. Indeed, I demonstrate that both Na_v blockers and Na_v-AEDs elicit neural tube defects when exposed to neurulating *Xenopus laevis* embryos. In addition, Na_v blockers and Na_v-AEDs comparably reduce neural plate cell calcium activity and reverse the developmental progression of neural plate cell calcium dynamics during neurulation suggesting that AEDs may inhibit calcium transients by impairing Na_v function. This work establishes FluoVolt™ membrane potential dye as a useful probe for studying neural plate cell resting membrane potential in *Xenopus*

laevis embryos and demonstrates that the resting membrane potential of neural plate cells is dependent on K^+, Na^+, and Cl^- gradients. Moreover, I find that Na_v blockers and Na_v-AEDs hyperpolarize neural plate cells. Here I propose a model of mechanisms of Na_v-AED induced NTDs. Resting membrane potential of neural plate cells allows for spontaneous activation of Na_v which in turn leads to further depolarization of neural plate cells and activation of NMDAR and calcium dynamics. This calcium activity is important for regulating neural plate cell cycle and neural tube formation. Na_v-AEDs interfere with Na^+ currents and calcium dynamics leading to NTDs. This work significantly contributes to the mechanistic understanding of neural activity regulating neural tube formation to advance the discovery of safer therapeutic options for pregnant women with epilepsy.

TABLE OF CONTENTS

Chapter I
Antiepileptic drugs and neural tube defects

1.1 Introduction

1.1.1 Neural tube formation

Vertebrate neurulation is a complex morphogenetic process occurring early in embryogenesis to form the neural tube, the prospective brain, and spinal cord (Figure 1.1.1). It requires highly choreographed sequential cellular and molecular events. Following the establishment of the three germ layers - endoderm, ectoderm, and mesoderm, a subset of ectodermal cells receive signals from the notochord to commit to neural fate (Harland, 2000; Borodinsky, 2017). This neural induction results in a dorsal thickening of the ectoderm referred to as the neural plate. Sequentially, the neural plate undergoes drastic cellular shape changes, including (1) apicobasal cell elongation to thicken and narrow the neuroepithelium and (2) mediolateral cell migration and intercalation to narrow the plate transversely while elongating the anteroposterior axis, a process known as convergent extension (Keller et al., 1992a,b,c; Davidson & Keller, 1999; Copp & Greene, 2013; Nikolopoulou et al., 2017). Neural plate bending and folding begins when the lateral edges of the plate rise to form neural folds (Davidson & Keller, 1999; Nikolopoulou et al., 2017). The folds elevate and converge until they fuse at the midline, which initiates radial intercalation between the two cell layers to form a single-layered closed neural tube (Edlund et al., 2013; Nikolopoulou et al., 2017; Borodinsky, 2017).

1.1.2 Xenopus laevis as a model organism to study neural tube formation

Xenopus laevis is a powerful amphibian model for studying vertebrate central nervous system development. In addition to the highly conserved cellular and molecular processes across vertebrates, *Xenopus laevis* has many attributes that make them

advantageous over other vertebrates. They have a sizeable oocyte with transparent eggshell that allows visualization and manipulation of early embryogenesis via simple approaches. Genetic engineering studies are made possible by the complete sequencing of the *Xenopus laevis* genome (Session et al., 2016). Non-invasive imaging approaches and simple microinjections of constructs into the developing embryo allow for manipulation of gene expression. In addition, neural plate folding and neural tube formation occur in a short period of 7 hours at 23ºC (Figure 1.1.1). Moreover, the developmental rate can be altered by growing embryos at various temperatures (Khokha et al., 2002; Nieuwkoop & Faber, 1994). Neurulation stages (stage 13, early neural plate, 15 hours post fertilization (hpf) at 23ºC through stage 20, early neural tube, 22 hpf at 23ºC) are well defined, with each stage identifiable by an unequivocal and characteristic external morphology corresponding to the progression of neural plate folding and neural tube formation (Nieuwkoop & Faber, 1994). Finally, while the central nervous system of *Xenopus laevis* is simpler than in higher vertebrates, many aspects of early development including the formation of the neural tube and generation of main neural cell types are highly conserved across vertebrates, supporting the use of this model for studies ranging from developmental mechanisms to drug discovery and toxicology (Borodinsky, 2017).

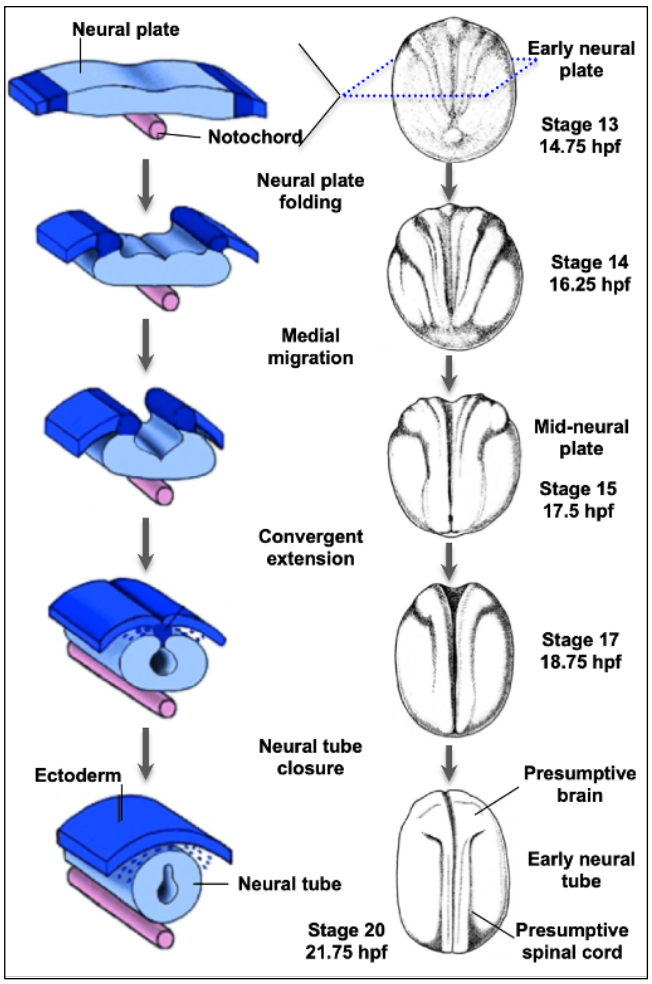

Figure 1.1.1. *Xenopus laevis* neural plate folding and neural tube closure time course (in hours post fertilization, hpf) (adapted from Nieuwkoop & Faber, 1994; Gilbert, 2000)

1.1.3 Neural tube defects

Neural tube defects (NTDs) are among the most common and debilitating congenital disabilities in the United States, occurring in 1 in 1,000 live births (Wallingford et al., 2013). NTDs are malformations of the brain, spine, or spinal cord associated with the failure of the neural tube to form and close properly. It is a heterogeneous phenotype defined by region-specific malformations, including (1) anencephaly, restricted to cranial

regions, (2) spina bifida of the caudal neural tube, and (3) craniorachischisis, which is embryonic lethal and extends across the entire body axis (Copp & Greene 2014).

Despite the prevalence and life-long patient impact, there is still little understood about NTD etiology. Hundreds of genes associated with the highly orchestrated operations of neural tube formation, such as cell adhesion and movement (Harris & Juriloff, 2010), cell polarity (Humphries et al., 2020), and DNA damage repair (Wallingford et al., 2013), have been identified in model systems to be associated with NTD risk. Studies have shown that patient-derived mutations of the core planar cell polarity gene VangI in *Drosophila* were causative of cell polarity defects, suggesting a potential causative relationship with resulting NTDs (Humphries et al., 2020). Nevertheless, no single gene mutation has been identified to cause human NTDs therefore they are considered multi-factorial disorders involving aberrant genetic and environmental interactions (Copp & Greene, 2013; Copp & Greene, 2014).

Decades of epidemiological data highlight several environmental factors as influencing the incidence of NTDs. Periconceptional supplementation with folic acid significantly reduces a woman's risk of an offspring with an NTD and is currently the primary preventative measure (Group et al., 1991; Berry et al., 1999; Blom et al., 2006). It is unclear how supplementation protects against a proportion of NTDs, mostly because folate is central to many cellular processes and why 30-50% of NTDs are not preventable (Blom et al., 2006). Maternal obesity and diabetes are well-recognized as complex risk factors for NTDs (Correa et al., 2003), as well as maternal fever and excessive use of hot tubs (Moretti et al., 2005). In addition, there is significant and increasing evidence of the

teratogenicity of antiepileptic drugs (AEDs) (Battino et al., 1992a,b; Kaneko et al., 1999; Kelly, 1984; Kelly et al., 1984a,b; Philbert & Dam, 1982; Wlodarczyk et al., 2012).

1.1.4 Antiepileptic drugs

Antiepileptic drugs (AEDs) treat various neurological disorders, including seizures, bipolar disorder, anxiety, and migraines (Sankaranen & Lachhwani, 2015; Wlodarczyk et al., 2012). AEDs decrease pathological hyperexcitability of the cerebral cortex via a multitude of primary targets and mechanisms of action (Falco-Walter, 2020; Kellogg & Meador, 2017). Seizures are disturbed brain functions resulting from abnormal electrical circuit excitation, affecting 10% of the global population (Falco-Walter, 2020). About 1 to 2% of the worldwide population, or 50 million people, have seizures due to epilepsy (Falco-Walter, 2020). Epilepsy is a neurological disorder defined by spontaneous and recurring seizures. There are various known etiologies of epilepsy, such as traumatic brain injury, brain tumors, congenital brain defects, stroke, liver and kidney failure, and idiopathic epilepsy (Falco-Walter 2020; Wlodarczyk et al., 2012). Without a cure, the goal is to manage the symptoms of this spontaneous and lifelong disorder. AEDs remain the primary treatment for reducing or eliminating seizures. Most people with epilepsy have well-controlled seizures, are otherwise healthy, and expect to participate in life experiences, including childbearing (Falco-Walter, 2020; Harden et al., 2009; Sankaranen & Lachhwani, 2015; Wlodarczyk et al., 2012).

1.1.5 Antiepileptic drugs and neural tube defects

Despite the effectiveness of AEDs for managing neurological disorders, their use in pregnant women with epilepsy has 50 years of alarming epidemiological evidence of increased risk of malformations. The risk of pregnancy resulting in an offspring with

significant congenital malformation doubles when compared to untreated pregnancies (Bangar, 2016; Battino et al., 1992a,b; Kaneko et al., 1999; Kellogg & Meador, 2017; Kelly, 1984; Kelly et al., 1984a,b; Philbert & Dam, 1982; Wlodarczyk et al., 2012). Valproic acid (VPA) and carbamazepine (CBZ) are the most widely used first-generation AEDs. They pose a reported 10- to 20-fold increased risk of offspring with NTDs over the general population (Bangar, 2016; Harden et al., 2009; Kallen, 1994; Kellogg & Meador, 2017; Little et al., 1993; Rosa, 1991; Wlodarczyk et al., 2012). The teratogenic mechanisms of AEDs are unknown. The prevailing paradigm is that AED-induced NTDs occur via off-target effects, including (1) inhibition of folate metabolism (Finnell et al., 2003; Wegner & Nau, 1992) (2) buildup of AED metabolites and oxidative stress (Morimoto et al., 2016; Pippenger, 2003) and (3) inhibition of histone deacetylases altering necessary gene expression and inhibiting cell proliferation necessary during rapid growth (Eyal et al., 2004; Gurvich et al., 2005). The role of AED primary targets in neural tube formation is commonly dismissed due to the mainstream belief that neural excitability is not apparent in early development. However, the evolving body of research supporting critical neural activity during early embryogenesis requires a closer look at AED molecular targets throughout neural tube formation (Blackshaw & Warner, 1976; Borodinsky & Spitzer, 2006, 2007; Goyal et al., 2020; Messenger & Warner, 1979; Sequerra et al., 2018).

1.1.6 Voltage-gated sodium channel-targeting antiepileptic drugs

For over 70 years, sodium channel blockers have been the pillar of epileptic pharmacological management. Voltage-gated ion channels regulate the flow of sodium (Na_v), potassium (K_v), or calcium (Ca_v) to control neuronal excitability. VPA, CBZ, lamotrigine (LTG), and phenytoin are drugs that modulate ion channel gating, blocking

high-frequency repetitive spike firing that occurs during a seizure without affecting ordinary neural activity (Rogawski & Loscher, 2004; Sankaranen & Lachhwani, 2015). These drugs act on action potential firing by preferential binding to the inactive conformations of the channels (Davies, 1995; Rogawski & Loscher, 2004; Sankaranen & Lachhwani, 2015). Phenytoin and CBZ are first-generation voltage-gated sodium channel AEDs (Na_v-AED) (Brodie, 2017). They are broad-spectrum, enzyme-inducing drugs with incredible efficiency in managing various seizures yet present complicated adverse effects and teratogenic warnings. The mission to develop safer and better-tolerated AEDs launched the second generation of Nav-AEDs, including LTG (Brodie, 2017; Sankaranen & Lachhwani, 2015). LTG possesses a wide range of efficacy, likely due to multiple mechanisms of action, including inhibition of Ca_V currents and enhancement of repolarizing K^+ currents (Brodie, 2017; Stefani et al., 1996; Zona et al., 2002). Women with epilepsy of childbearing ages are strongly recommended to rely on a therapy regimen consisting of second-generation Na_v-AEDs due to the reported increased safety profile (Brodie, 2017; Sankaranen & Lachhwani, 2015; Stefani et al., 1996; Zona et al., 2002). The question remains whether the safety of these new AEDs is due to improved mechanisms or the inherent lack of years of epidemiological data. It is of utmost importance to study first and second-generation AEDs in tandem to improve our understanding of the mechanisms that underly the teratogenic effects.

In this chapter, I test the hypothesis that exposure to Na_v-AEDs during neurulation induces NTDs in *Xenopus laevis* embryos. I define the dose-response relationship between Na_v-AEDs and the incidence of NTDs by exposing neurulating *Xenopus laevis* embryos to

clinically relevant concentrations (Arfman et al., 2020; Falco-Walter, 2020; Ohman et al., 2000; Patsalos et al., 2018). In addition, I assess the severity, histological and cellular phenotypes of AED-induced NTDs in *Xenopus laevis* embryos.

1.2 Materials and Methods

1.2.1 Animals

Mature oocytes were collected from *Xenopus laevis* females previously injected with human chorionic gonadotropin hormone. *In vitro* fertilization was performed by exposing the oocytes to a small piece of minced testis in a dish with 10% Marc's Modified Ringers (MMR) saline solution containing (mM): 10 NaCl, 0.2 KCl, 0.1 $MgSO_4$, 0.5 HEPES, 5 EDTA, and 0.2 $CaCl_2$. This defined time 0 of fertilization. Fertilized embryo jelly coats were partially removed by incubation with 2% cysteine solution (pH 8) followed by 10% MMR washes. Embryos were grown in 10% MMR at 23ºC. Animals were handled under an approved Institutional Animal Care and Use Committee protocol and guidelines.

1.2.2 AED Incubations

Fertilized embryos were grown to neural plate stages (stage 13, 15 hpf) for pharmacological incubations. At that point, they were incubated with 0.001 – 2 mM carbamazepine (CBZ, Sigma-Aldrich, catalog # C4024), 0.001 – 2 mM lamotrigine (LTG, Sigma-Aldrich, catalog # L3791), vehicle (10% MMR/0.05% DMSO) or control (10% MMR) from stage 13 until control embryos exhibit a closed neural tube (stage 20, 22 hpf). Incubations were at 23ºC.

1.2.3 Immunohistochemistry

Embryos (stage 20 - 22) were fixed with 2% trichloroacetic acid (TCA) for 1 h at 23ºC or with 4% paraformaldehyde (PFA) for 2 h or 30 min at 4ºC or 23ºC, respectively. Fixed embryos were processed for immunostaining (Balashova et al., 2017; Belgacem & Borodinsky, 2015) and standard protocols for paraffin embedding and 10-μm transverse sectioning. Antigen retrieval was performed by microwaving sections in 0.05% citraconic anhydride (pH 7.4). 4% BSA was used for blocking and 0.1% Tween-20 was added to antibody and washing solutions. Primary and secondary antibody incubations were done overnight at 4ºC and 2 h at 23ºC, respectively. Primary antibodies included: anti-Sox2, 1:500 (catalog # AF2018, R&D Systems), anti-E-cadherin 5D3, 1:50 (Developmental Studies Hybridoma Bank at the University of Iowa, Iowa City, IA), and anti-alpha Tubulin, 1:500 (catalog # ab15246, Abcam). Secondary antibodies included Alexa Fluor™ conjugated 488 (catalog # A-21202, Invitrogen) , 568 (catalog # A-11057, Invitrogen) and 647 (catalog # A-31573, Invitrogen).

1.2.4 Assessment of neural tube defect incidence and severity

AEDs (0.001 – 2 mM), vehicle (0.05% DMSO), and saline (10% MMR) groups were scored for NTD incidence and severity. Incidence was reported as the percent of embryos per treatment group exhibiting the failed neural fold convergence phenotype at the midline ($N > 6$ independent experiments, $n \geq 30$ embryos per group). Nuclei in transverse sections (10-μm, 70 sections average per stage 20 – 22 embryo) were labeled with DAPI. NTD severity was determined by counting the number of sections exhibiting opened and closed neural tube and reported as percent of sections per embryo with open neural tube ($N > 3$ independent experiments, $n \geq 6$ embryos per group).

1.2.5 Assessment of neural tube morphological and histological abnormalities

Transverse sections (10 μm, stage 20 – 22) were labeled with DAPI, anti-Sox2, anti-E-cadherin, and anti-alpha tubulin using the immunohistochemistry methodology previously mentioned. Control (10% MMR), vehicle (10% MMR / 0.05% DMSO), 0.1 – 0.5 mM LTG and 0.1 – 0.5 mM CBZ incubated embryos were assessed for morphological and histological abnormalities. Neural tube width was measured using a measuring tool within ImageJ ($N \geq 3$ independent fertilizations, n = 5 embryos/group, n = 3 medial sections/embryo). The number of Sox2+ and DAPI+ cells in the neural tube per 5 medial sections per embryo ($N \geq 3$, n = 8 embryos per group) was quantified using Olympus cellSens imaging and analysis software. A defined neural tube Region of Interest (ROI) was traced per sample. Independent fluorescent thresholds were defined as twice the background for both channels. The minimum object size was set to 100-pixels. These parameters remained consistent among independent samples. Cell counts were generated based on thresholded binary transformation within the ROI.

1.2.6 Statistical analysis

Nonlinear fit analysis with three or four parameters and a confidence level of 95% was employed to analyze incidence and severity data sets ($N \geq 6$ independent experiments, $n \geq 30$ embryos). Extra sum-of-squares F Test was used to compare the EC_{50} values between groups to identify if there was a significant difference in experimental compared to control. For cell count data, ANOVA or Student's t-test followed by Tukey's post hoc test evaluated significance ($N \geq 3$ independent experiments, $n \geq 8$ embryos). Differences were considered significant when $p<0.05$.

1.3 Results

1.3.1 AEDs induce NTDs in a dose-dependent manner

Neurulating *Xenopus laevis* embryos were incubated in CBZ or LTG for the extent of neural tube formation (stage 13 – 20, 15 – 22 hpf). Clinically relevant concentrations of Nav-AEDs (0.001 – 2 mM) (Arfman et al., 2020; Falco-Walter, 2020; Ohman et al., 2000; Patsalos et al., 2018) were used in six independent fertilization batches of embryos. Treatments were paired with appropriate controls, including embryos incubated with saline (10% MMR) and vehicle (0.05% DMSO in 10% MMR). Incubations were done at 23ºC. When control embryos had reached 22 hpf and neural tube closure was complete, I scored the number of embryos from each group that presented a NTD or lack of fusion at the dorsal midline and the total number of embryos (Figure 1.3.1A).

Incubation of embryos with either of the Na_v-AEDs, CBZ or LTG leads to an increase in the incidence of NTDs in a concentration-dependent manner (Figure 1.3.1B). The fitting of dose-response curves reveals that the potency of CBZ is significantly higher than that of LTG (CBZ EC_{50} = 0.88 mM; LTG EC_{50} = 1.32 mM; Figure 1.3.1B). Nevertheless, they both elicit 100% NTDs at 2 mM dose.

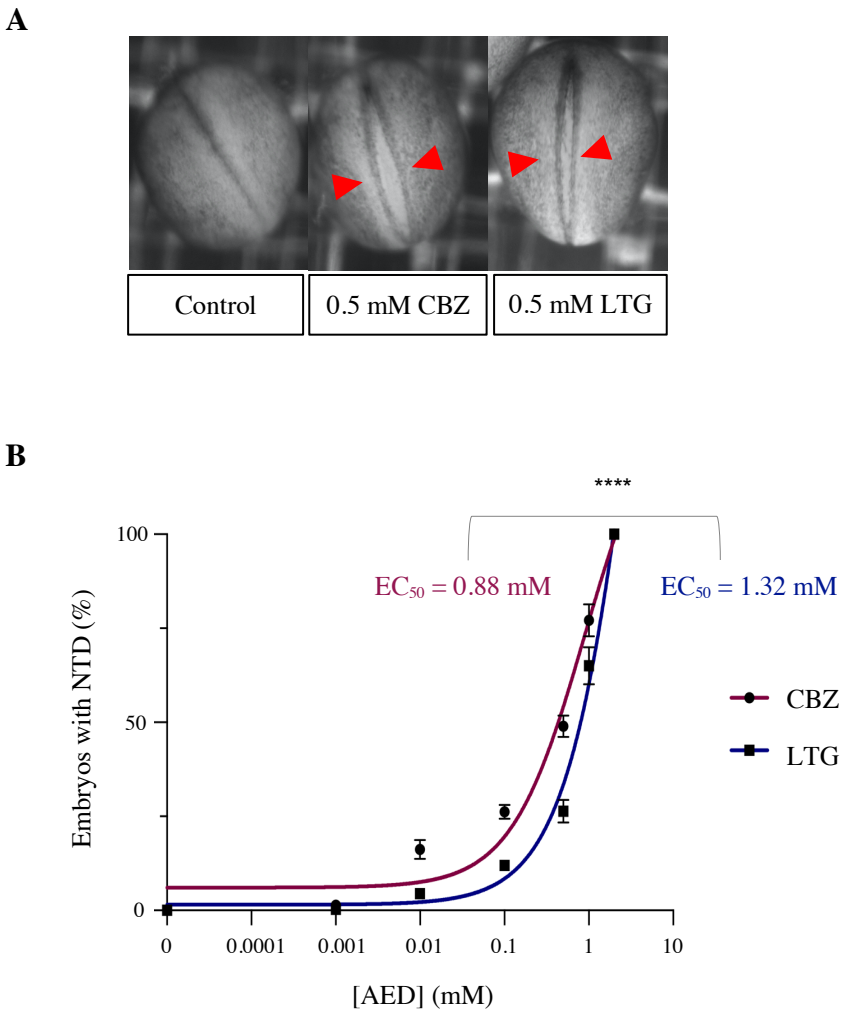

Figure 1.3.1. AEDs induce NTDs in a dose-dependent manner. Embryos were incubated in either vehicle (0.05% DMSO), 0.001 to 2 mM carbamazepine (CBZ) or lamotrigine (LTG) during neurulation (7 h, stage 13 through 20). **A,** Representative micrographs of stage-20 whole-embryos from each group incubated with vehicle (Control), 0.5 mM CBZ or 0.5 mM LTG. Arrowheads indicate the NTDs. **B,** Incidence of NTDs was assessed as the percent of embryos with an open neural tube, n ≥ 30 embryos per group, N ≥ 6 independent experiments. Data points represent mean±SEM, curves represent nonlinear fit with three (CBZ, R^2 0.97) or four (LTG, R^2 0.98) parameters with confidence level 95%, EC_{50}: the concentration causing malformations in 50% of the embryos. Extra sum-of-squares F Test to compare the EC50 values of CBZ and LTG, $F_{1,65}$ = 18.45, ****p<0.0001.

1.3.2 CBZ has higher teratogenic potency than LTG

With the evidence that CBZ and LTG cause NTDs in a dose-dependent manner, I sought to assess the severity of the NTDs. The embryos that were incubated in either vehicle (0.05% DMSO) or 0.001 to 2 mM carbamazepine (CBZ) or lamotrigine (LTG) during neurulation (7 h, stages 13 through 20) were fixed and processed for transverse sectioning and nuclear labeling with DAPI. The severity of NTDs was assessed by counting the 10-μm-thick sections from the entire anteroposterior axis of the embryo that exhibit an open neural tube (Figure 1.3.2A). This is clinically relevant as human NTDs are categorized by the location and extent of the defect along the central nervous system axis (Copp & Greene, 2014). The EC_{50} defines the concentration of the AED that causes malformations in 50% of the sections per embryo (Figure 1.3.2B). When comparing EC_{50} values (CBZ EC_{50} = 0.16 mM; LTG EC_{50} = 1.37 mM; Figure 1.3.2B), CBZ is significantly ($p<0.0001$) more potent at producing severe NTDs than LTG.

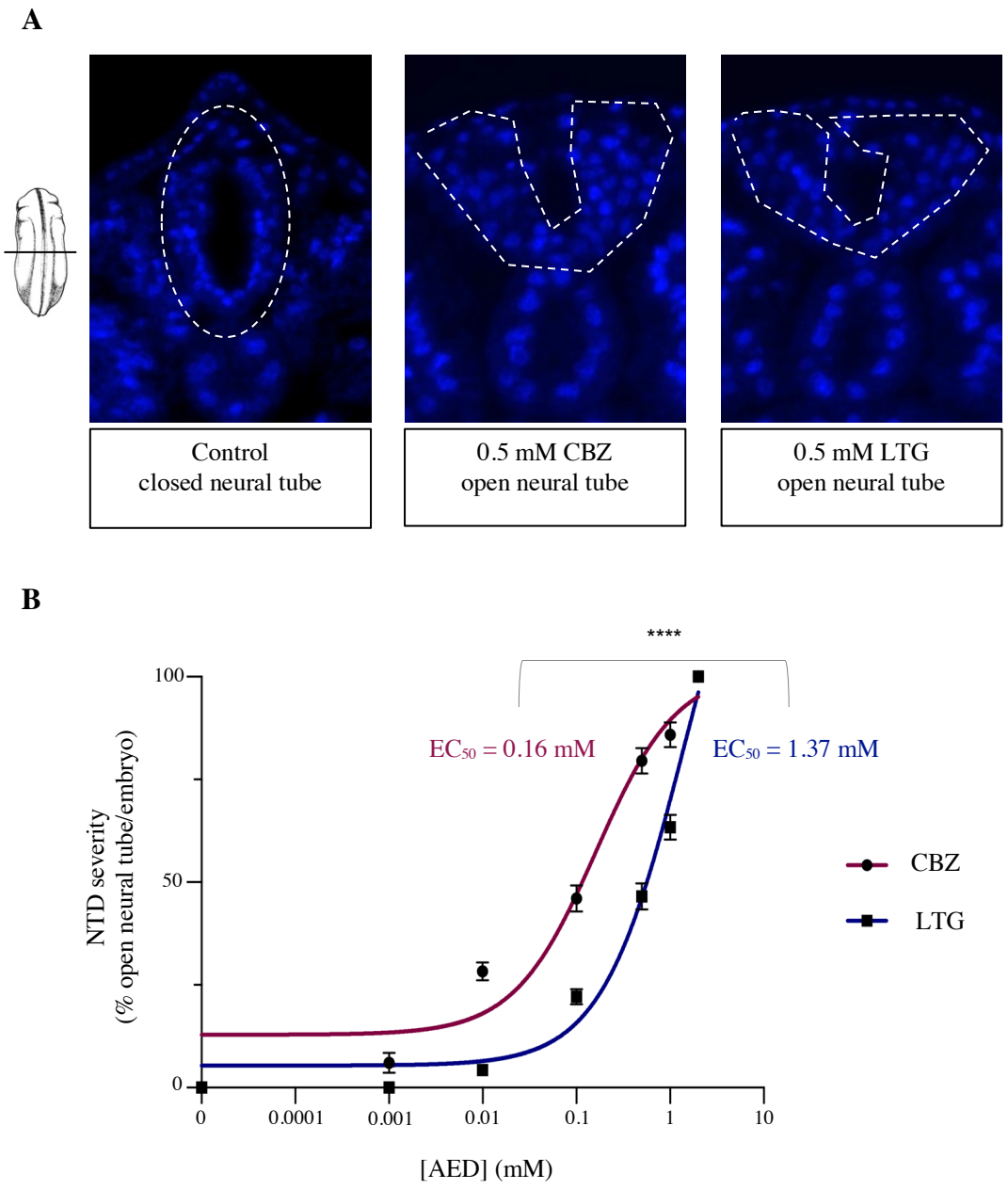

Figure 1.3.2. CBZ has higher teratogenic potency than LTG. Embryos were incubated in either; vehicle (0.05% DMSO control 0 mM), 0.001 to 2 mM carbamazepine (CBZ) or lamotrigine (LTG) during neurulation (7 h, stage 13 through 20), when they were fixed and processed for transverse sectioning and nuclear labeling with DAPI. Severity of NTDs was assessed by counting the number of 10-μm -thick sections from the entire anteroposterior axis of the embryo that exhibit an open neural tube. **A,** Representative transverse sections of embryos (stage 20) from each group. White tracing shows a closed neural tube (control) versus open neural tube (CBZ and LTG). **B,** Data points represent mean±SEM percent of sections with open neural tube. Curves represent nonlinear fit with three parameters, R^2 0.92 with confidence level 95%. N $\geq$ 3 independent experiments, n $\geq$ 6 embryos per group. EC_{50}: the AED concentration causing malformations in 50% of the sections per embryo. Extra sum-of-squares F Test to compare the EC50 values of CBZ and LTG, $F_{1,80}$ = 32.60, ****p<0.0001.

1.3.3 AED exposure during neurulation results in alterations in neural tube morphology

Both CBZ- and LTG-exposed embryos present with a neural tube that was thicker in appearance than that of the control (Figure 1.3.3A). The measuring of three medial sections per embryo revealed that both 100, 500 μM CBZ- or 500 μM LTG-exposed embryos have a thicker neural tube (Figure 1.3.3B). Additionally, it was observed that the cellular organization of AED-exposed embryos differed from that of the control (Figure 1.3.3A). Sox2+ neural stem cells line the lumen of the newly closed neural tube in control embryos, while neural progenitors and differentiating neurons (Sox2-immunonegative cells) position in outer regions of the neural tube (Figure 1.3.3A). In contrast in AED-exposed embryos, Sox2+ cells can be identified throughout the defective neural tube (Figure 1.3.3A). These findings suggest that AED exposure interferes with the normal progression of neural stem cell differentiation in the neural tube.

A

Sox2 / E-Cadherin / α tubulin / DAPI

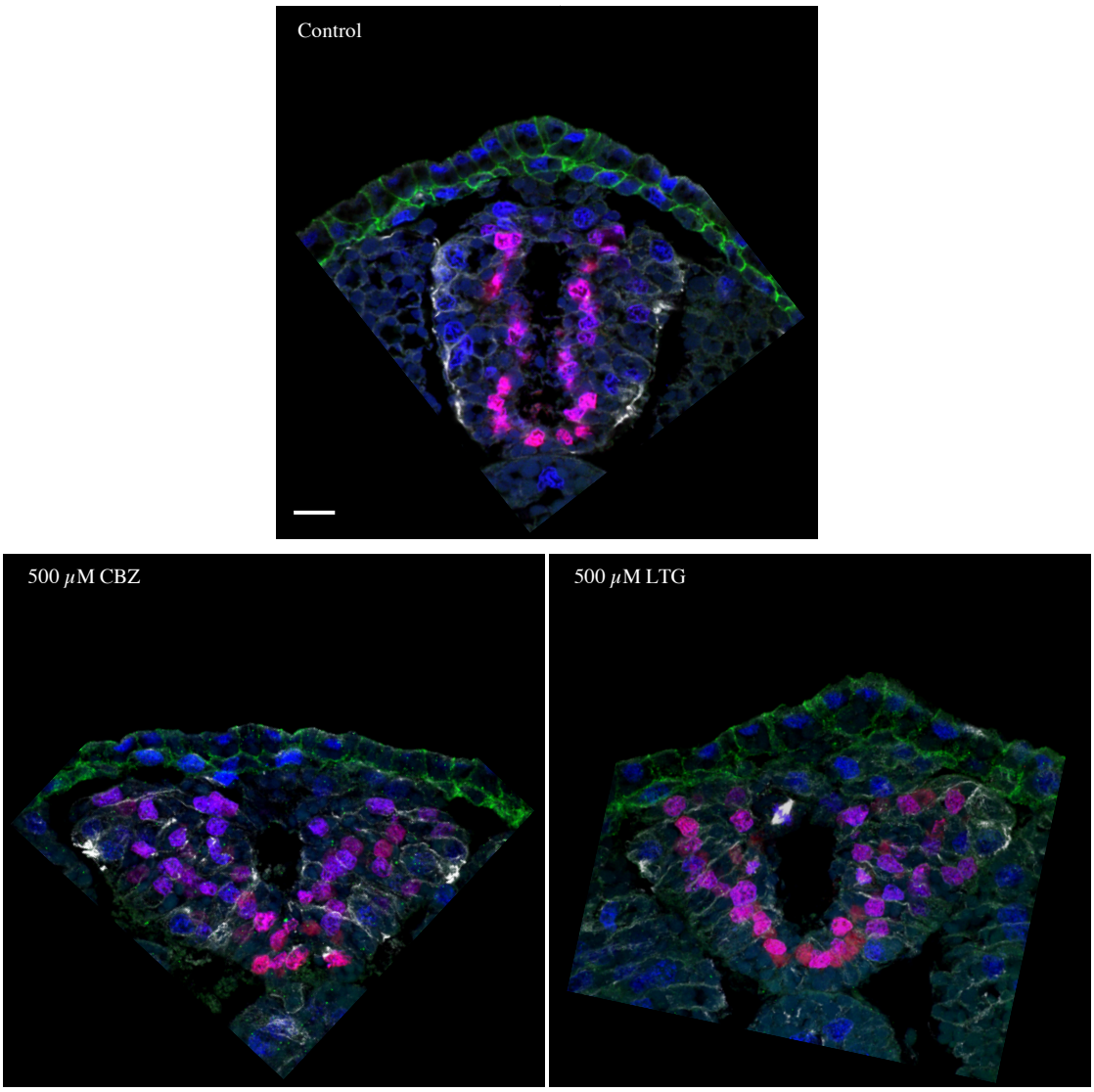

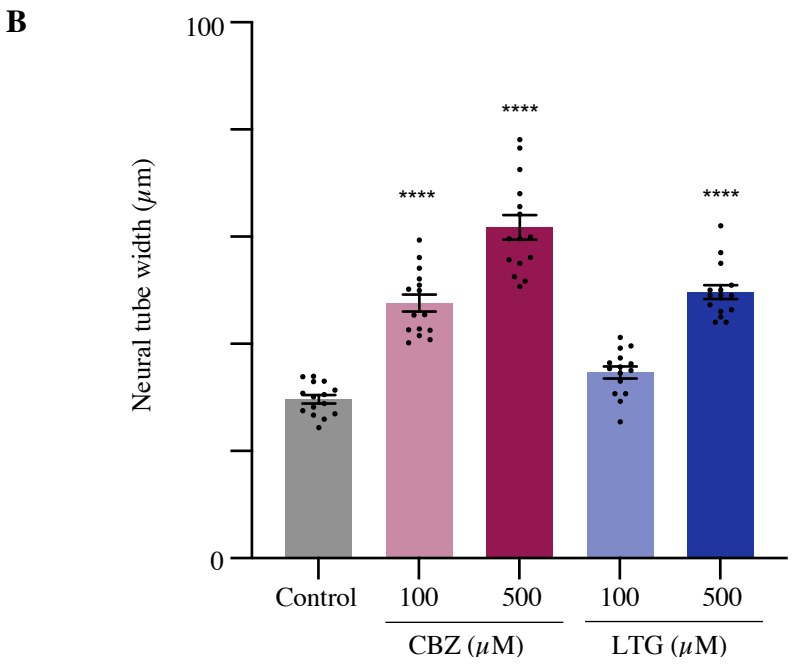

Figure 1.3.3. AED exposure during neurulation results in alterations in neural tube morphology. Embryos were incubated in either vehicle (0.05% DMSO control 0 μM), or 100 μM to 500 μM carbamazepine (CBZ) or lamotrigine (LTG) during neurulation (7 h, stage 13 through 20). Embryos from each group were fixed and processed for transverse sectioning (10 μm-thick), nuclear labeling (DAPI) and immunostaining for neural stem cell marker (Sox2), non-neural ectoderm marker (E-Cadherin) and alpha-tubulin. **A,** Representative transverse sections of embryos (stage 20) incubated with vehicle (control), 500 μM CBZ or LTG. Neural ectoderm can be identified by Sox2+ cells. Scale bar = 20 μm **B,** Shown is mean$\pm$SEM medial neural tube width in transverse (10-μm) sections; N = 3, n = 5 embryos/group; n = 3 medial sections/embryo, ****p<0.0001, 1-way ANOVA followed by Tukey's test to compare control to treatment groups.

1.3.4 AED exposure during neurulation increases the number of cells in the neural tube

The neural tube of embryos incubated with 100 μM to 500 μM CBZ or LTG during neurulation (7 h, stage 13 through 20) are mediolaterally thicker compared with controls (Figure 1.3.4A). Therefore I sought to determine if there was a significant difference in the number of cells in the AED treated groups. Embryos from each group were fixed and processed for transverse sectioning (10 μm-thick) and nuclear labeling (DAPI) and immunostaining for neural stem cells (Sox2) (Figure 1.3.4A).

The neural ectoderm was identified by Sox2+ cells and used as the ROI (Figure 1.3.4A). The number of DAPI+ and Sox2+ cells in 500 μM CBZ and LTG neural tubes were significantly higher than in control samples (Figure 1.3.4A,B). The ratio of Sox2+ to DAPI+ cells in the neural tubes of 500 μM CBZ- and LTG-treated embryos was significantly higher than that of controls and embryos exposed to lower concentrations of the AEDs (Figure 1.3.4A-C).

A

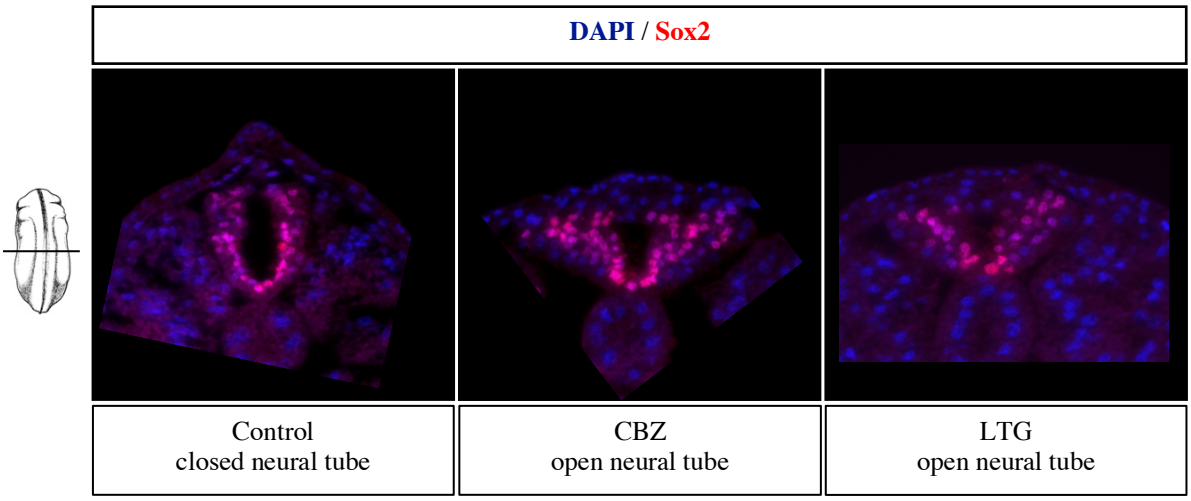

B

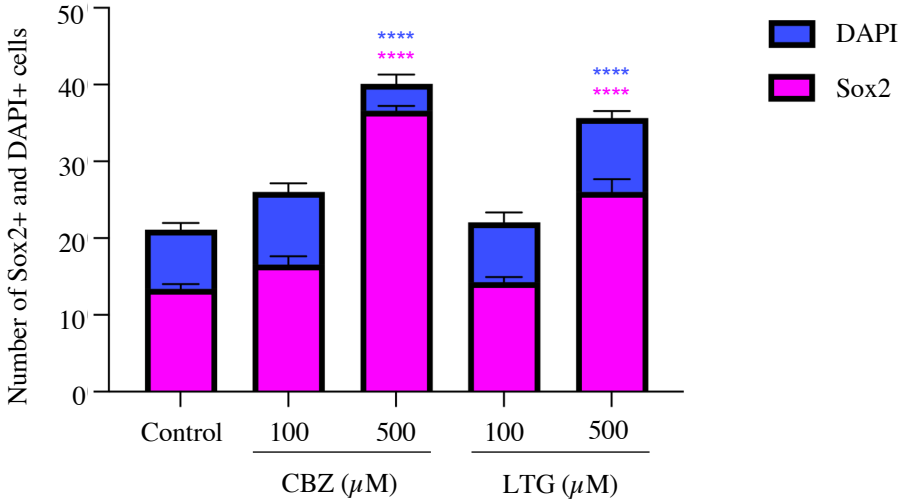

C

	Ratio Sox2+ : DAPI+ cells
Control	0.62
100 μM CBZ	0.65
500 μM CBZ	0.93****
100 μM LTG	0.64
500 μM LTG	0.76*

Figure 1.3.4. AED exposure during neurulation increases the number of cells in the neural tube. Embryos were incubated in either vehicle (0.05% DMSO control), or 100 μM to 500 μM carbamazepine (CBZ) or lamotrigine (LTG) during neurulation (7 h, stage 13 through 20). Embryos from each group were fixed and processed for transverse sectioning (10 μm-thick) and nuclear labeling (DAPI) and immunostaining for neural stem cell marker (Sox2). **A,** Representative transverse sections of embryos (stage 20) incubated with vehicle (control), 500 μM CBZ or LTG. Neural ectoderm can be identified by Sox2+ cells. **B,** Number of Sox2+ and DAPI+ cells in the neural tube per 10-μm transverse section; n = 8 embryos/group; n = 5 medial sections/embryo, mean±SEM, ****p<0.0001, 1-way ANOVA followed by Tukey's test to compare control to treatment groups for each labeled cell. **C,** Ratio of Sox2+ to DAPI+ cells in the neural tube of control- and 100 μM to 500 μM CBZ- or LTG-treated groups, n = 8 embryos per group, *p<0.05, ****p<0.0001 1-way ANOVA followed by Tukey's test compared with control.

1.4 Discussion

The use of first-generation AEDs during pregnancy is associated with an increased risk of congenital disabilities in offspring, yet much less is known about newer generation AEDs in this respect. Therefore, further studies such as this are critical to compare AEDs at different dosages to assess the teratogenic potential of newer generation AEDs. With the surge of new-generation AEDs approved and deemed safe for pregnancy, there is an urgency to better understand the effects on fetal development to predict risk rather than wait for decades of epidemiological data.

CBZ has a long history of teratogenic evidence. Many years of studies and epidemiological data have concluded first-trimester exposure to CBZ increases malformations such as NTDs, craniofacial defects, developmental delays, and cognitive changes (Holmes et al., 2001; Kuo, 1997, 1998; Morimoto et al., 2005; Nie et al., 2016; Ornoy, 2009; Patsalos et al., 2018, Pippenger, 2003). GlaxoSmithKline (London, UK) began a database of women on LTG in 1992, which revealed a 2- to 3-fold increase in fetal malformations (Cunnington & Tennis, 2005; Nie et al., 2016). Another UK database suggests that LTG teratogenic effects are dose-dependent, with a higher risk for women on

an LTG polytherapy. The database reports that pregnant women with epilepsy on LTG had a 5-fold greater risk of having a newborn with a facial cleft versus untreated women, creating further concern as to the actual gestational safety of LTG (Nie et al., 2016; Tennis & Eldridge, 2002).

This study demonstrates that CBZ is a highly potent teratogen in *Xenopus laevis*, eliciting severe NTDs at the lowest clinically relevant concentration, similar to what is seen in humans (Banger, 2016; Harden et al., 2009; Hiilesmaa, 1992; Holmes et al., 2001; Kallen, 1994; Kaneko et al., 1999, Kellogg & Meador, 2017; Kelly, 1984; Little et al., 1993; Nie et al., 2016; Pippenger, 2003; Rogawski & Loscher, 2004; Rosa, 1991; Sankaranen & Lachhwani, 2015) validating the use of this model to investigate the mechanisms underlying the AED-induced NTDs and suggesting that these mechanisms may be conserved across species. In addition, the incidence and severity of LTG-induced NTDs in *Xenopus laevis* embryos are dose-dependent. We also observed a dose-dependent thickening of the neural plate in CBZ or LTG exposed embryos. Further investigation revealed that AED exposure increased the overall number of cells in the neural tube, with higher doses significantly increasing neural progenitor cells. The control neural tubes transition away from the stem cell fate to progress into neuronal differentiation, but the AED groups maintained the "stemness" phenotype. These data align with previous studies exploring the association of increased neural cell proliferation with NTDs (Keller-Peck & Mullen, 1997; Patterson et al., 2014; Sequerra et al., 2018; Wu et al., 2001). The overexpression of transcription factor Tumorhead in *Xenopus laevis* causes increased neural cell proliferation and impaired neural plate bending and neuronal differentiation (Wu et al., 2001). Studies with rodent models of spina bifida have reported increased cell

proliferation in the posterior neural tube (Keller-Peck & Mullen, 1997) and NTDs resulting from the disruption of neuronal cell cycle progression and differentiation in the early stages of neurulation (Patterson et al., 2014). The precise regulation of cell proliferation and differentiation is critical to the success of neural tube formation, and this study provides evidence that AEDs disrupt these processes.

The findings of this chapter spotlight the importance of exploring the mechanisms of action underlying the teratogenic effects of CBZ and LTG. Our findings support the model that LTG presents a significant increase in the risk of NTDs, and its current safety profile, in comparison to other AEDs, is likely due to the lack of epidemiological data (Cunnington & Tennis, 2005; Nie et al., 2016; Tennis & Eldridge, 2002). Despite the associated danger, these drugs are frequently prescribed during pregnancy due to the importance of therapeutically controlling seizures in pregnant women. The overall goal of uncovering the teratogenic mechanisms of AEDs is to develop a new generation of drugs that protects the mother from epileptic symptoms and diminishes the danger to the offspring.

Chapter II:
Voltage-gated sodium channels during neurulation

2.1 Introduction

2.1.1 Neural activity during early embryogenesis – neurotransmitters

The mainstream paradigm of neural tube formation is that it is strictly coordinated by genetic programming, and electrical activity is not present in these early stages of development prior to establishing synapses. However, studies continue to provide evidence of neurotransmitter activity during the early stages of embryogenesis (Borodinsky, 2004; Borodinsky & Spitzer, 2006, 2007; Goyal et al., 2020; LoTurco et al., 1995; Root et al., 2008; Sequerra et al., 2018; Smith & Walsh, 2020).

Neurotransmitters and neurotransmitter receptors are expressed during neurulation (Kapur et al., 1991; Lauder et al., 1981; Root et al., 2008; Rowe et al., 1993), regulating neural cell proliferation and migration (Rowe et al., 1993). GABA, glutamate, dopamine, and noradrenaline are expressed in the medial-posterior neural plate of *Xenopus laevis* embryos (Root et al., 2008; Rowe et al., 1993). The presence of these neurotransmitters prior to synapse formation suggests non-synaptic mechanisms of neurotransmission (Borodinsky, 2014; Goyal et al., 2020; Sequerra et al., 2018). Recent studies have shown glutamatergic signaling throughout neural tube formation (Sequerra et al., 2018). When glutamate signaling is inhibited, there is an increase in proliferative cells in the neural plate (Sequerra et al., 2018). Glutamate signaling, in part through NMDA receptors, activates calcium dynamics during neurulation (Sequerra et al., 2018). Glutamate-mediated calcium signaling is essential for regulating neural plate stem cell proliferation and migration, as the disruption of this signaling results in NTDs (Sequerra et al., 2018).

Calcium is one of the most potent second messengers in biology. Unlike many other second messengers, it cannot be metabolized, therefore the tight regulation of extracellular to intracellular movement is critical. The ability to control intracellular calcium concentration and location is pivotal for regulating various cell functions. Not surprisingly, electrical activity during neurulation relies on calcium dynamics (Goyal et al., 2020; Sequerra et al., 2018). Presumably a conserved feature of developmental biology, calcium-mediated electrical activity has been identified during embryonic spinal cord development in mouse (Hanson & Landmesser, 2003), rat (Ren & Greer, 2003), chick (Sernagor et al., 1995; Chub & O'Donovan, 1998; O'Donovan et al., 1998), *Xenopus laevis* (Gu et al., 1994; Gu & Spitzer, 1995; Borodinsky et al., 2004), *Xenopus tropicalis* (Marek et al., 2010) and zebrafish (Warp et al., 2012; Plazas et al., 2013). Neurotransmitters induce calcium transients resulting in cytoskeleton remodeling of developing neurons (Zheng & Poo, 2007). Similar changes in cell shape and movement are necessary during neural tube formation. Studies have shown calcium influx activates neural-specific genes essential for neural induction, driving cells to neural fate (Moreau et al., 2008).

The medial neuroectoderm of *Xenopus laevis* exhibits spontaneous transients in intracellular calcium concentration, and these transients increase in frequency with the progression of neural plate folding (Sequerra et al., 2018). Neural plate cell calcium activity is partially mediated by NMDA receptors (Sequerra et al., 2018) and T-type calcium channels (Abdul-Wajid et al., 2015). Interestingly, the AED valproic acid (VPA) inhibits calcium activity in the neural plate, comparable to the effects seen when inhibiting NMDA receptors, resulting in neural tube defects (NTDs) (Sequerra et al., 2018). The NMDA receptor blockade- and VPA-induced NTDs can be rescued by enhancing ERK 1/2

activation. Moreover, VPA-induced NTDs can be partially rescued by preincubating embryos with NMDA, suggesting that VPA induces NTDs by interfering with glutamate signaling necessary for neural tube formation (Sequerra et al., 2018). Given the relevance of neural activity, neurotransmitters and Ca^{2+} dynamics in presynaptogenic stages of the nervous system development, it is important to consider the primary targets of AEDs as the mechanisms underlying AEDs teratogenicity by assessing their effect on neural activity during neural tube formation.

2.1.2 Neural activity during early embryogenesis – ion channels and membrane potential

Ion conductance in the mature nervous system is the basis of neurotransmission. Synaptic function and neuronal excitability are dependent on the expression and gating mechanisms of various ion channels. However, the role of ion channels prior to the establishment of synapses and throughout neural tube formation is still unclear. In *Xenopus laevis* the expression of voltage- and neurotransmitter-gated ion channels is evident in neural stem cells as early as neural plate stages (Abdul-Wajid et al., 2015; Goyal et al., 2020; Sequerra et al., 2018; Spencer et al., 2019).

Studies have shown that sodium current is essential to neural differentiation (Messenger & Warner, 1979; Pai et al., 2015; Robinson & Stump, 1984). The folding neural plate of *Xenopus laevis* presents an ionic current pattern consisting of Na^+-dependent inward current stronger in the mid-lateral neural plate which decreases near the midline of the neural groove (Robinson & Stump, 1984). A similar mediolateral current pattern was identified and disrupted by the overexpression of $K_v1.5$ and subsequent incubation with a chloride channel agonist. This disruption of the putative ionic currents resulted in defects in brain morphogenesis (Pai et al., 2015).

Neural plate stage *Xenopus laevis* embryos exposed to strophanthidin, a Na^+/K^+ ATPase inhibitor, display a reduction in neural differentiation and ultimately a 50% reduction in white matter of the mature nervous system (Messenger & Warner, 1979). In addition, increasing extracellular potassium during the strophanthidin treatment protects differentiating neurons from the inhibitory effects of the cardiac glycoside, suggesting that the activation of the sodium pump is essential to neural differentiation (Messenger & Warner, 1979). Furthermore, the mean resting membrane potential of neural plate cells of axolotl embryos increases when embryos enter mid-neural plate stages of development (Blackshaw & Warner, 1975). Increasing extracellular potassium during this spontaneous resting membrane potential change causes the neural plate cells to hyperpolarize (Blackshaw & Warner, 1975). Both the spontaneous increase in resting membrane potential and the potassium-induced hyperpolarization of neural plate cells can be prevented by the addition of cardiac glycosides, suggesting that the sodium pump is functional following neural induction (Blackshaw & Warner, 1975).

Given the established presence of sodium currents in neural plate cells and the importance of sodium to neural differentiation (Blackshaw & Warner, 1975; Messenger & Warner, 1979; Pai et al., 2015; Robinson & Stump, 1984) it is important to consider channels that potentially contribute to sodium flux during neural plate stages. Scn1a is the gene that codes for the alpha subunit of voltage-gated sodium channels (Na_v). Scn1a transcripts have been identified in the neural plate of *Xenopus laevis* embryos in early neurulation (stage 13) with expression levels that increase throughout neural plate folding (Sessions et al., 2016). Sodium channel-blocking antiepileptic drugs (Na_v-AEDs) operate in the mature nervous system by binding to the alpha subunit of Na_v (Yip et al., 2014). The

spatiotemporal expression, localization, and function of Na_v during neural plate folding and neural tube development have yet to be investigated.

In this chapter, I test the hypothesis that voltage-gated sodium channels (Na_v) are expressed during neurulation and essential to neural tube formation. I discover the spatiotemporal presence of Na_v in *Xenopus laevis* embryos during neural tube formation. Furthermore, I demonstrate the relevance of Na_v during neural tube formation by utilizing Na_v blockers to assess the consequences to neural plate cell calcium dynamics, resting membrane potential, and neural tube formation.

2.2 Materials and Methods

2.2.1 Animals

Mature oocytes were collected from *Xenopus laevis* females previously injected with human chorionic gonadotropin hormone. *In vitro* fertilization was performed by exposing the oocytes to a small piece of minced testis in a dish with 10% Marc's Modified Ringers (MMR) saline solution containing (mM): 10 NaCl, 0.2 KCl, 0.1 $MgSO_4$, 0.5 HEPES, 5 EDTA, and 0.2 $CaCl_2$. This defined time 0 of fertilization. Fertilized embryo jelly coats were partially removed by incubation with 2% cysteine solution (pH 8) followed by 10% MMR washes. Embryos were grown in saline (10% MMR) at 23ºC. Animals were handled under an approved Institutional Animal Care and Use Committee protocol and guidelines.

2.2.2 Na_v blocker incubations

Fertilized embryos were grown to neural plate stages (stage 13, 15 hours post-fertilization (hpf)) in saline (10% MMR) at 23ºC. Subsequently, they were incubated with 0.02% tricaine

methanesulfonate (TMS, Sigma-Aldrich, catalog # E10521), 0.0001% tetrodotoxin citrate (TTX, catalog # 1069, Tocris), 0.05% DMSO in 10% MMR vehicle for TTX or saline (10% MMR, vehicle for TMS) from stage 13 until control embryos exhibit a closed neural tube (stage 20, 22 hpf). Incubations were at 23ºC.

2.2.3 Immunohistochemistry

Embryos (stage 20 - 22) were fixed with 2% trichloroacetic acid (TCA) for 1 h at 23ºC or with 4% paraformaldehyde (PFA) for 2 h or 30 min at 4ºC or 23ºC, respectively. Fixed embryos were processed for immunostaining (Balashova et al., 2017; Belgacem & Borodinsky, 2015) and standard protocols for paraffin embedding and 10-μm transverse sectioning. Antigen retrieval was performed by microwaving sections in 0.05% citraconic anhydride (pH 7.4). Tween-20 was added to antibody and washing solutions. Primary and secondary antibody incubations were done overnight at 4ºC and 2 h at 23ºC, respectively. Primary antibodies included: anti-Pan-Na_v1, 1:500 (clone N419/40, catalog # 75-405, UC Davis/NIH NeuroMab Facility), anti-Sox2, 1:500 (catalog #AF2018, R&D Systems); anti-E-cadherin 5D3, 1:50 (Developmental Studies Hybridoma Bank at the University of Iowa, Iowa City, IA); and anti-alpha Tubulin, 1:500 (catalog #ab15246, Abcam). Secondary antibodies included Alexa Fluor™ conjugated 488 (catalog # A-21202, Invitrogen) , 568 (catalog # A-11057, Invitrogen) and 647 (catalog # A-31573, Invitrogen).

2.2.4 Assessment of neural tube defect incidence and severity

Incidence of NTDs was quantified as the percent of embryos per treatment group exhibiting the failed neural fold convergence phenotype at the midline (N > 3 independent experiments, n ≥ 30 embryos per group). Groups included; 0.02% TMS, 0.0001% TTX, 0.05% DMSO, and saline (10% MMR). Nuclei in transverse sections (10-μm, 70 sections average per stage 20 –

22 embryo) were labeled with DAPI. NTD severity was determined by counting the number of sections exhibiting opened and closed neural tubes and reported as the percent of sections per embryo with an open neural tube (N > 3 independent experiments, n ≥ 6 embryos per group).

2.2.5 Western blot assay

Whole embryos (stages 13, 17 or 20) were homogenized in an extraction buffer containing: 20 mM Hepes (pH 7.4), 5 mM EDTA, 20 mM NaCl, and protease inhibitors (Thermo Scientific, Catalog # 784115). Samples were put on ice for 10 min with vortexing every 3 min then centrifuged at 16,100 rpm for 10 min at 4ºC. The pellet (nuclear fraction) was stored at -80 ºC for future processing. The supernatant (cytosolic and membrane fractions) was removed and centrifuged at 16,000 rpm for 30 min at 4ºC. The supernatant (cytosolic fraction) was removed and boiled with Laemmli buffer to prepare for running a 10% SDS-PAGE. The pellet (membrane fraction) was washed three times with extraction buffer at 16,000 rpm for 20 min each wash to remove residual cytosolic proteins. Following washes, the sample was boiled with Laemmli buffer. Both cytosolic and membrane fraction samples were run on a 10% SDS-PAGE followed by transferring to PVDF membrane. Protein transfer to PVDF membrane was done overnight at 4ºC. The PVDF membrane was probed with anti-Pan-Na_v1, 1:500 (clone N419/40, catalog # 75-405, UC Davis/NIH NeuroMab Facility), and the cytosolic protein phopsho-p38 MAP Kinase 1:1,000 (Cell Signaling Technology, catalog # 9211) antibodies in 5% BSA. PVDF membranes were stripped in 0.2 M glycine HCl buffer, pH 2.5, 0.05% Tween for 20 min. The membranes were then probed using the membrane marker anti-α1 subunit sodium-potassium ATPase antibody 1:1,000 (Abcam, catalog # ab767) and the cytosolic protein p38α MAP Kinase 1:1,000 (Cell Signaling Technology, catalog # 9228) antibodies in

5% BSA. HRP-conjugated secondary antibodies 1:10,000 (Jackson ImmunoResearch) in 1% BSA were incubated for 10 min and visualized by the ECL+ substrate developing kit (Thermo Scientific, catalog # 32106) on a BioRad imager.

2.2.6 Calcium imaging with Na_v blockers

DNA for the genetically-encoded Ca^{2+} sensor GCaMP6s (pGP-CMV-GCaMP6s was a gift from Douglas Kim & GENIE Project (Addgene plasmid # 40753 ; http://n2t.net/addgene:40753 ; RRID:Addgene_40753) (Chen et al., 2013)) was subcloned into $pCS2^+$ vector. The restriction sites for Bg1II and NotI were included in the $pCS2^+$ vector using the forward primer 5'-TCACTAAAGGGAACAAAAGATCTGGGTACCGGGCCCAA-3' and the reverse primer 5'-TTGGGCCCGGTACCCAGATCTTTTGTTCCCTTTAGTGA-3'. mRNA for injections into *Xenopus laevis* embryos was *in vitro* transcribed from the plasmid using the mMessage mMachine (Ambion) standard protocol and kits. Two- to four-cell stage embryos previously dejellied were injected with GCaMP6s mRNA (0.8 – 1 ng per embryo). Embryos were incubated with 6% Ficoll in 10% MMR for 1 h post-injection and grown to neural plate stages in saline (10% MMR). Neural plate stage embryos 16 – 19 hpf were imaged using a Sweptfield confocal microscope (Nikon) at an acquisition rate of 0.1 Hz for a total of 35 min. Imaging per embryo consisted of a control period (0-5 min, in 10% MMR) and a treatment period (5-35 min, treatment solution). A single embryo was situated for dorsal midline imaging by using clay in an imaging dish with saline (10% MMR). Following the 5 min control period of imaging, TMS or TTX was added to the imaging dish to achieve the desired treatment concentration. As in previous studies, calcium transients were detected by a peak change in fluorescence of at least twice the level of the noise (Belgacem and Borodinsky, 2011; Borodinsky et al., 2004; Borodinsky and Spitzer, 2007; Sequerra et al., 2018; Swapna

and Borodinsky, 2012; Tu and Borodinsky, 2014; (Figure 2.3.3)). Calcium transients were quantified at various time periods (0-5, 5-10, and 30-35 minutes). The number of calcium transients for each treatment period was compared to the control period to assess the percent change in calcium transients over time. Significance was determined by one-way ANOVA followed by Tukey's multiple comparisons test.

2.2.7 Membrane potential sensor incubation

Xenopus laevis embryo jelly coats were partially removed by incubation with 2% cysteine solution (pH 8) followed by saline (10% MMR) washes. Two-cell stage embryos (1.5 hpf) were injected with membrane mCherry mRNA (mCherry-Mem was a gift from Narasimhan Gautam (Addgene plasmid #36075; http://n2t.net/addgene:36075; RRID: Addgene_36075) (Chisari et al., 2009). Embryos were incubated with 6% Ficoll in 10% MMR for 1-hour post-injection and grown to neural plate stages in saline (10% MMR). When embryos reached stage 13 - 14 (15 – 16 hpf), they were incubated with FluoVolt™ Membrane Potential dye (FluoVolt™ Membrane Potential Kit, catalog # F10488, ThermoFisher) using a 1:10 solution of FluoVolt dye (488) to Powerload Concentrate Loading Buffer with probenecid (catalog # P36400, ThermoFisher). Embryos were incubated with the FluoVolt™ solution for 30 min, protected from light at 23ºC. Embryos were subsequently washed three times with saline (10% MMR) and maintained at 23ºC (Figure 2.3.5).

2.2.8 Imaging of changes in resting membrane potential in the presence of different extracellular ion concentrations and Na_v blockers

Xenopus laevis neural plate stage embryos (16 – 19 hpf) expressing mCherry-Mem and previously loaded with FluoVolt™ Membrane Potential Dye were imaged using a Sweptfield confocal microscope (Nikon) at an acquisition rate of 0.1Hz for 15 min with the 488 and 568 lasers. A single embryo was situated for dorsal midline imaging by using clay in an imaging

dish with saline (10% MMR). Each embryo was imaged for a control period (0-5 min) and a treatment period (5-15 min). After the 5 min control period, 250 μL of various stock solutions were added to image the following groups; (1) KCl (0.2 – 2 mM), (2) NaCl (10 – 100 mM), (3) Na^+ gluconate (10 – 100 mM), (4) 0.02% TMS, (5) 0.0001% TTX, (6) sucrose (40 – 200 mM), (7) saline (10% MMR) ($N \geq 5$, $n \geq 4$ per group). The percent change in fluorescence intensity (AU) over time of FluoVolt™ was normalized using the mCherry-Mem fluorescent intensity (Figure 2.3.5). The data is reported as the mean$\pm$SEM percent change in FluoVolt and mCherry-Mem ratio ($N \geq 3$, $n \geq 5$).

2.2.9 Statistical analysis

ANOVA evaluated significance, followed by Tukey's post hoc multiple comparisons test. $N \geq 3$ independent fertilizations and $n \geq 6$ embryos per group for all data sets unless specifically indicated. Differences were considered significant when $p<0.05$.

2.3 Results

2.3.1 Na_v are present during neurulation and localize to the membrane of neural plate cells during neural plate folding

To investigate the spatiotemporal expression of Na_v during neural tube formation, I prepared cytosolic and membrane fractions from embryo cell lysates for western blot assays. I detect Na_v1 expression in the cytosol fraction of early (stage 13) neural plate stage embryos, whereas the Na_v1 protein from mid-late neural plate stage embryos (stage 15 - 20) was detected in the membrane fraction (Figure 2.3.1A). The expression and localization of Na_v1 were confirmed by immunohistochemistry (Figure 2.3.1B). The neural plate of *Xenopus laevis* consists of two layers of neural plate cells, the superficial and deep, and Na_v appears in the cytosol of both layers at early neural plate stages, stage 13 (Figure

2.3.1B). Na_v is membrane-associated in neural plate cells from mid-late neural plate stage embryos (Figure 2.3.1B). Newly differentiated neurons line the periphery of the neural tube as revealed by the enrichment in α-tubulin from specialized microtubules essential to neuronal differentiation (Aiken et al., 2017). The α-tubulin-enriched cells on the periphery of the neural tube are associated with high levels of Na_v immunolabeling (Figure 2.3.1C), confirming the specificity of Na_v immunolabeling in neural plate stages. Therefore, increased expression and membrane localization of Na_v is associated with maturing neurons in the newly closed neural tube (Figure 2.3.1C). These results indicate that Na_v is expressed by *Xenopus laevis* neural plate cells throughout neural plate folding and neural tube closure and its insertion in neural plate cell membranes increases with the progression of neural tube formation (Figure 2.3.1). These findings suggest that Na_v may play an important role in this process.

A

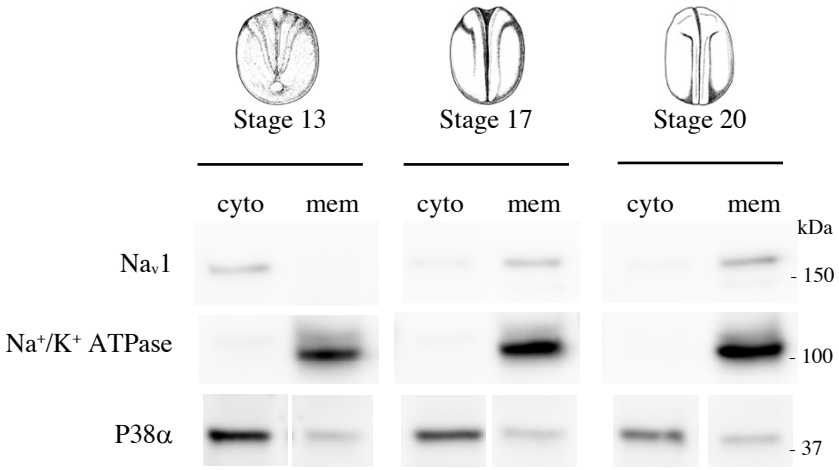
Stage 13
Stage 17
Stage 20
cyto
mem
cyto
mem
cyto
mem
kDa
Nav1
- 150
Na+/K+ ATPase
- 100
P38α
- 37

B

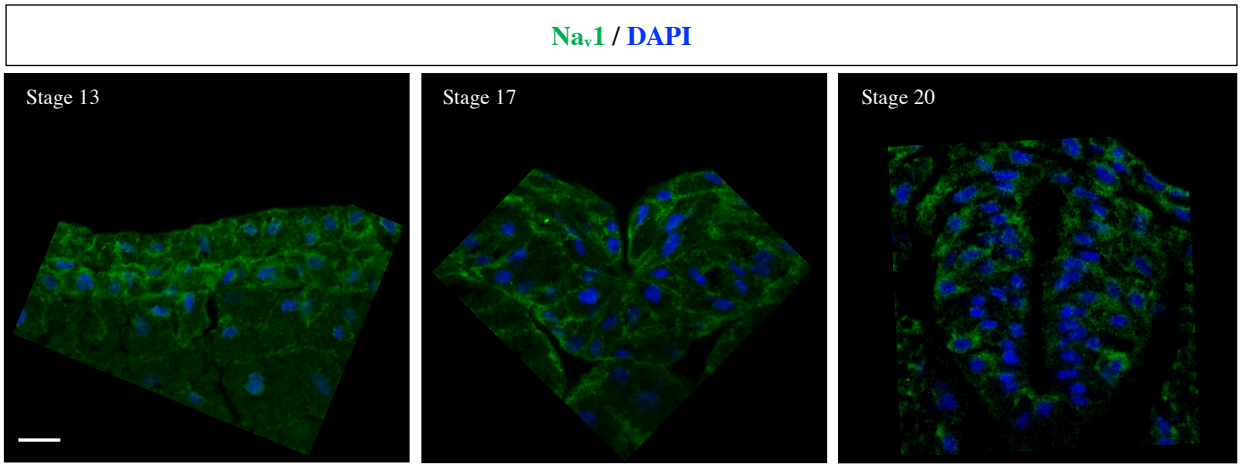
Nav1 / DAPI
Stage 13
Stage 17
Stage 20

C

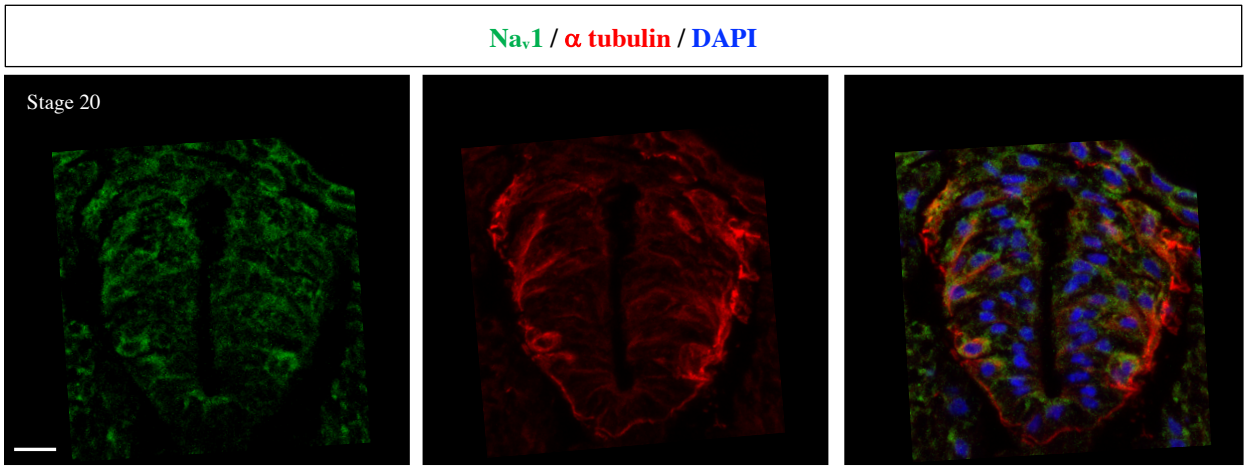
Nav1 / α tubulin / DAPI
Stage 20

Figure 2.3.1. Na_v are present during neurulation and localizes to neural plate cell membrane during neural plate folding. A, Western blot assay from cytosolic and membrane fractions prepared from lysates from neural plate stage *Xenopus laevis* embryos at stage 13, 17 and 20 (Nieuwkoop & Faber, 1994). **B-C,** Immunostained 10 μm-thick transverse sections from stage 13, 17 or 20 embryos. Scale bar: 20 μm.

2.3.2 Na_v blockers induce NTDs

To investigate the function of Na_v during neural tube formation *Xenopus laevis* embryos were incubated with either TMS or TTX throughout neurulation (stage 13 – 20). The exposure of either 0.02% TMS or 0.0001% TTX during neural tube formation resulted in NTDs (Figure 2.3.2). TMS exposure during neural tube formation resulted in a higher NTD incidence and severity when compared to TTX exposure (Figure 2.3.2B). TMS is a mainstream anesthetic for fish and amphibians as it blocks the activity of both sensory and motor nerves (Ramlochansingh et al., 2014). TMS is structurally similar to benzocaine and blocks the generation of action potentials by reversibly interacting with the central cavity of Na_v via non-specific hydrophobic interactions (Martin and Corry, 2014; Ramlochansingh et al., 2014). Studies have attributed the potent inhibitory effects of TMS to the direct access route from the lipid bilayer through the hydrophobic pocket (Martin and Corry, 2014). On the other hand, TTX is a uniquely structured peptide that binds to the outer pore of Na_v specifically through guanidinium and hydroxyl groups to occlude sodium permeation into the cell (Lee and Ruben, 2008). Therefore, it is possible that the higher NTD incidence and severity caused by TMS compared with TTX is due to the differences in binding properties and accessibility to deeper cells in the neural tissue. Moreover, Na_v binding affinity for TTX is greatly affected by changes in electrostatic

interactions between TTX and the amino acids lining the pore, giving rise to variations in TTX-sensitivity (Lee and Ruben, 2008). In addition, since TTX is a large peptide its access to the embryo is likely diminished by the embryo's jelly coat, reducing the penetration of the drug to the neural plate.

A

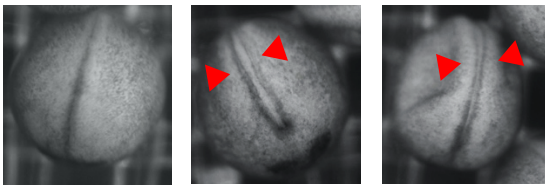

B

	NTD incidence (average % embryos with open neural tube)	NTD severity (average % open neural tube/embryo)
Control (10% MMR)	1%	13%
0.02% TMS	35%	79%
0.0001% TTX	11%	48%

Figure 2.3.2. Na_v blockers induce NTDs. Embryos were incubated with either saline (control), 0.02% TMS, or 0.0001% TTX during neurulation (7 h, stage 13 through 20) when they were fixed and processed for transverse sectioning and nuclear labeling with DAPI. **A,** Representative micrographs of stage-20 whole-embryos from each group incubated with saline (Control), 0.02% TMS, or 0.0001% TTX. Arrowheads indicate the NTDs. **B,** Incidence of NTDs was assessed as the percent of embryos with an open neural tube, $N \geq 6$ independent experiments, $n \geq 60$ embryos per group. Severity of NTDs was assessed by counting the number of 10-μm -thick sections from the entire anteroposterior axis of the embryo that exhibit an open neural tube, $N \geq 3$ independent experiments, $n \geq 6$ embryos per group.

2.3.3 Calcium dynamics are present during neurulation

To assess the presence of and changes in calcium dynamics during *Xenopus laevis* neurulation I employed the genetically encoded calcium indicator GCaMP6s (Chen et al., 2013). GCaMP6s mRNA was injected into two- or four-cell stage embryos and when embryos reached mid-neurulation (stage 15) time-lapse *in vivo* imaging was used to measure calcium dynamics. Imaging was done for a total of 35 min with a 5 min control period and 30 min treatment period (Figure 2.3.3A). Calcium transients were scored over three 5 min periods throughout the imaging window to compare the percent change in transients detected over time (Figure 2.3.3A). Neuroectodermal cells exhibit spontaneous calcium transients (Figure 2.3.3B). The calcium transients were quantified when the change in GCaMP6s fluorescence intensity at the peak was twice that of the noise (Figure 2.3.3C), as previously reported (Belgacem & Borodinsky, 2011; Borodinsky et al., 2004; Borodinsky & Spitzer, 2007; Sequerra et al., 2018; Swapna & Borodinsky, 2012; Tu & Borodinsky, 2014). My findings show that embryos incubated with vehicle (0.05% DMSO) or saline exhibit a comparable change in the number of calcium transients within the 35 min recording consisting in a steady increase in calcium transient frequency as neural plate folding progresses (Figure 2.3.4).

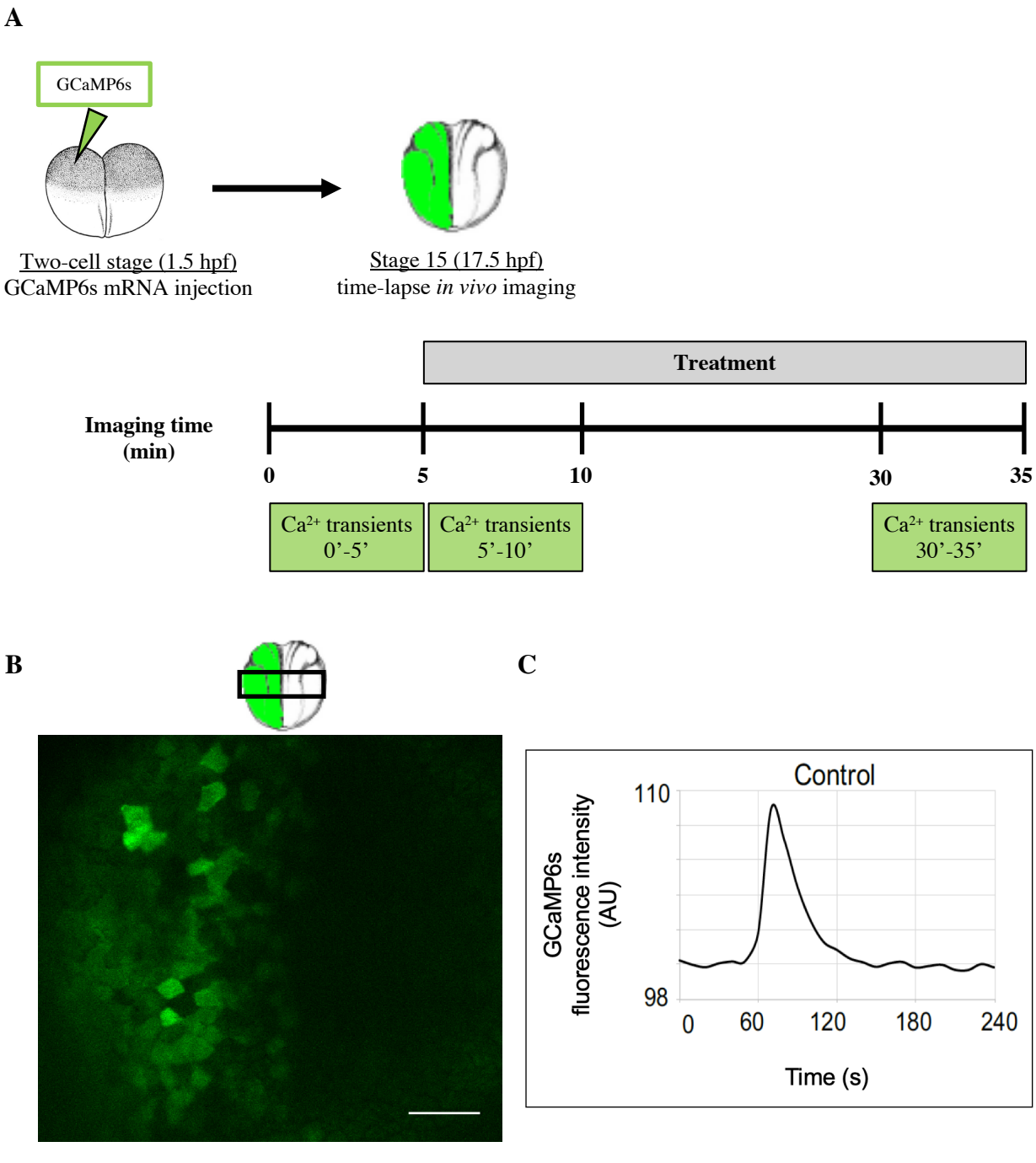

Figure 2.3.3. Ca^{2+} dynamics are present during neurulation. A, Schematic of Ca^{2+} imaging experimental design. Two-cell stage *Xenopus laevis* embryos were unilaterally injected with GCaMP6s mRNA. At stage 15, intact embryos were time-lapse *in vivo* imaged for 35 min. Treatment was added after 5 min of imaging and number of Ca^{2+} transients were measured at the indicated time windows. hpf: hours post-fertilization at 23°C (Nieuwkoop and Faber, 1994). **B,** Representative image of stage 15 unilaterally GCaMP6s-expressing embryo. Scale bar: 100 μm **C.** Representative trace of *in vivo* spontaneous Ca^{2+} transient in a neural plate cell from a neurulating embryo. Transients were scored if change in fluorescence was at least double the noise.

2.3.4 Na_v blockers reverse the developmental progression of calcium dynamics of neural plate cells during neurulation

Xenopus laevis embryos exposed to either TMS or TTX during neurulation resulted in diminished neural plate cell calcium dynamics detected by the genetically-encoded calcium sensor GCaMP6s (Figure 2.3.4). Within the first 5 min of exposure, both Na_v blockers were effective in reducing calcium activity (Figure 2.3.4). Over 30 min, Na_v blockers reverse the normal developmental progression of calcium activity during neural tube formation (Figure 2.3.4). TMS caused a greater reduction in calcium activity when compared to the effect of TTX exposure (Figure 2.3.4). Altogether these results indicate that Na_v are important for enabling calcium dynamics in the neural plate necessary for neural plate folding and neural tube formation.

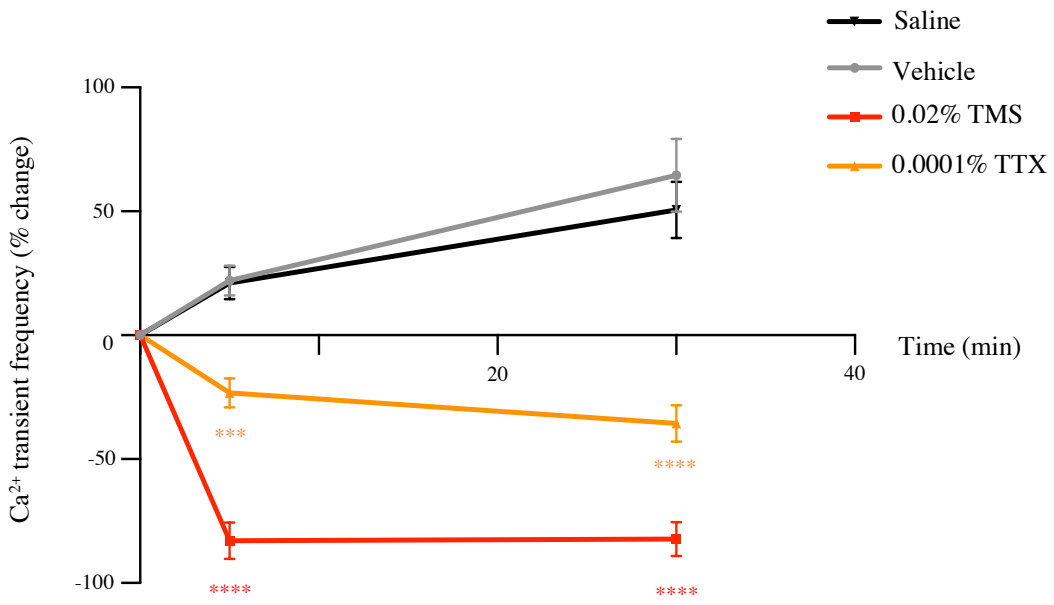

Figure 2.3.4. Na_v blockers reverse the developmental progression of Ca^{2+} dynamics of neural plate cells during neurulation. Ca^{2+} transients were detected by time-lapse *in vivo* imaging whole embryos (stage 15, 17.5 hpf) expressing the GCaMP6s Ca^{2+} sensor. Embryos were incubated in either saline (n = 12), vehicle (0.05% DMSO, n = 30), 0.02% TMS (n = 8) or 0.0001% TTX (n = 8). Percent change was calculated by comparing the number of transients detected 5 min before starting the incubation with drugs or vehicle or saline to the number of transients detected at both 5 min and 30 min following the addition of the treatment. N ≥ 3 independent experiments, mean±SEM, ***p<0.001, ****p<0.0001, one-way ANOVA followed by Tukey's multiple comparisons test to compare vehicle or saline to treatment groups.

2.3.5 Method for assessing changes in neural plate cell resting membrane potential using FluoVolt, a voltage-sensitive dye

FluoVolt™ (FV) is a member of the VoltageFluor family of fluorescent sensors that detect voltage changes by modulation of photo-induced electron transfer from an electron donor through a synthetic molecular wire to a fluorophore (Ceriani and Mammano, 2013). FV is an electrophysiological and optical approach to visualizing and quantifying connectivity in cell networks coupled by gap junctions (Ceriani and Mammano, 2013). It is advantageous because it is easy to load, gentle on the sample, and compatible with

standard imaging equipment (FITC emission/excitation settings). *Xenopus laevis* embryos injected with mCherry-Mem and incubated with FV sensor developed normally, while other membrane potential probes caused malformations.

Two-cell stage *Xenopus laevis* embryos were bilaterally injected with mCherry-mem mRNA to account for changes in membrane fluorescence intensity independent of a change in membrane potential, for example, because of movement or changes in cell shape. Embryos were grown to neural plate stages and incubated in FV membrane potential dye at stage 14. Embryos were subsequently time-lapse *in vivo* imaged to assess changes in neural plate cell resting membrane potential (Figure 2.3.5 A). The mCherry-mem signal normalized the FV signal to report the percent change in FV to mCherry-mem fluorescence intensity (Figure 2.3.5 B-C). An increase in fluorescence intensity indicates depolarization of the membrane, such as the effects seen when extracellular K^+ concentration is increased (Figure 2.3.5 B-C), while a decrease is caused by hyperpolarization. FluoVolt™ (FV) membrane potential dye is an effective reporter for studying neural plate cell resting membrane potential during *Xenopus laevis* neural tube development (Figure 2.3.5).

A

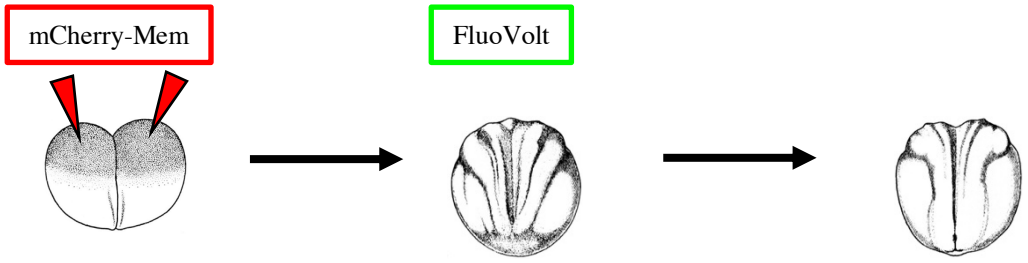

Two-cell stage (1.5 hpf)
mCherry-Mem mRNA injection

Stage 14 (16.25 hpf)
Incubate in FluoVolt Dye for 30 min

Stage 15 (17.5 hpf)
time-lapse *in vivo* imaging

B

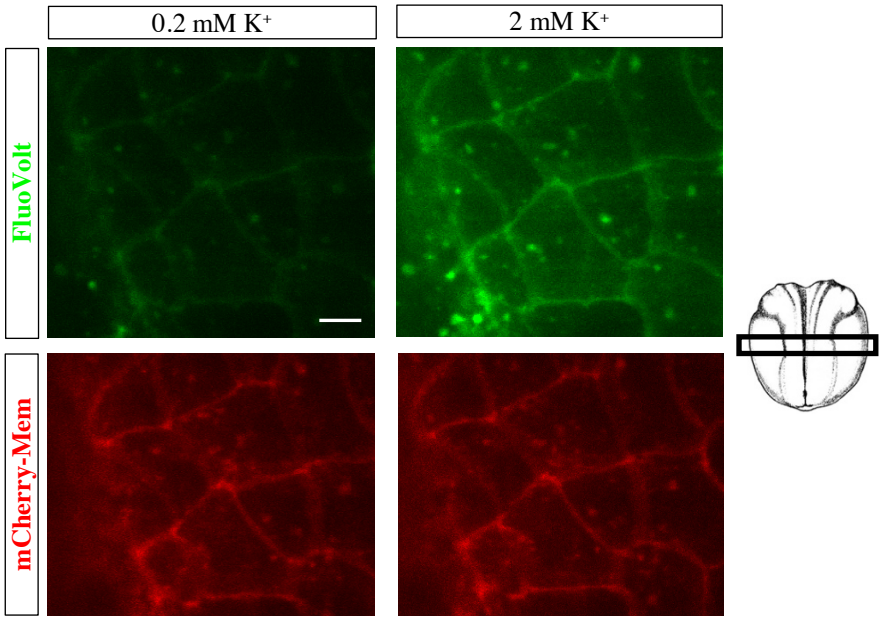

C

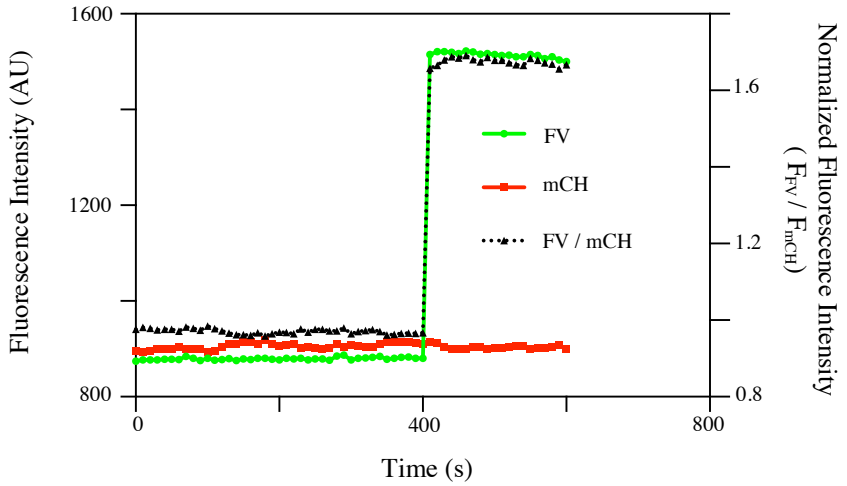

Figure 2.3.5. Method for assessing changes in neural plate cell resting membrane potential using FluoVolt, a voltage sensitive dye. Two-cell stage *Xenopus laevis* embryos were bilaterally injected with the membrane reporter mCherry (mCherry-Mem) mRNA. Neural plate stage embryos (stage 14-15) expressing mCherry-Mem were incubated with the voltage-sensitive dye FluoVolt. mCherry-Mem was used to normalize the FluoVolt fluorescence intensity. Embryos were time-lapse imaged with an acquisition rate of 0.1 Hz before and after the addition of various treatments. **A.** Schematic of experimental design. **B.** Representative images of neural plate before and after the addition of 2 mM K^+, scale bar 10 μm. **C.** Traces represent changes in fluorescence intensity (AU) for FluoVolt (green) and mCherry-Mem (red) and ratio of FluoVolt over mCherry-Mem signal (black) over time.

2.3.6 Resting membrane potential of neural plate cells is dependent on K^+, Na^+ and Cl^- gradients

The FluoVolt™ (FV) membrane potential dye was used to investigate the effects of ions on the resting membrane potential of *Xenopus laevis* neural plate cells. mCherry-Mem (mCH)-expressing neural plate stage embryos were loaded with FV (Figure 2.3.5). *In vivo* time-lapse imaging was employed to capture the effects of increasing the extracellular concentration of various ions on the resting membrane potential of neural plate cells (Figure 2.3.6). The FV intensity increased by 2-fold in the presence of 2 mM K^+, indicating that neural plate cells depolarized (Figure 2.3.6). Increasing the extracellular concentration of Na^+ depolarized neural plate cells (Figure 2.3.6). In addition, 100 mM Cl^- hyperpolarized neural plate cells (Figure 2.3.6). The FV signal response to the indicated ions was reproducible across five experiments (independent fertilizations). The addition of 40-200 mM sucrose did not elicit a change in FV fluorescence intensity, suggesting that FV fluorescence changes in response to changes in extracellular ion concentrations is independent of changes in osmolarity. These findings suggest that the resting membrane potential of neural plate cells is dependent on K^+, Na^+ and Cl^- gradients.

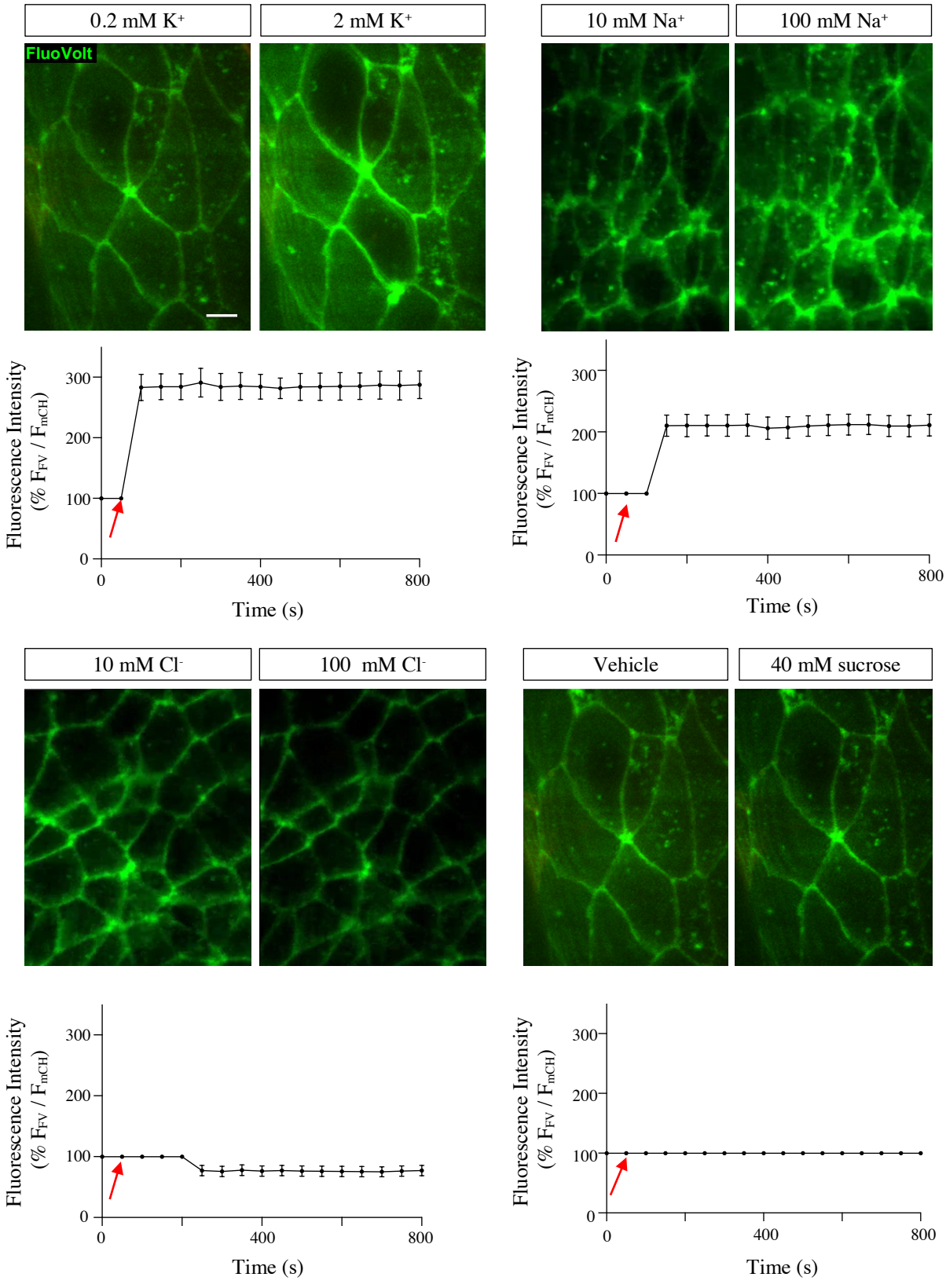
0.2 mM K+
2 mM K+
FluoVolt
10 mM Na+
100 mM Na+
Fluorescence Intensity
(% FFV / FmCH)
300
200
100
0
0
400
800
Time (s)
10 mM Cl-
100 mM Cl-
Vehicle
40 mM sucrose

Figure 2.3.6. Resting membrane potential of neural plate cells is dependent on K^+, Na^+ and Cl^- gradients. Neural plate stage embryos (stage 15 to 17) expressing mCherry-Mem were incubated with the voltage-sensitive dye FluoVolt™. Embryos were time-lapse imaged with an acquisition rate of 0.1 Hz before and after the addition of 2 mM K^+, 100 mM Na^+, or 100 mM Cl^-. Sucrose was used as an osmolarity control. Shown are representative images of neural plate before and after the addition of indicated solutions, scale bar 10 μm. Traces represent the mean $\pm$SEM percent change in FluoVolt (FV) / mCherry-Mem (mCH) ratio over time, $N \geq 5$, $n \geq 5$, red arrow shows the addition of the indicated solution.

2.3.7 Na_v blockers hyperpolarize neural plate cells

I investigated the effects of Na_v blockers on the resting membrane potential of *Xenopus laevis* neural plate cells. Both 0.02% TMS and 0.0001% TTX hyperpolarize neural plate cells, identified by a reduction in the ratio of FV to mCH signal intensity (Figure 2.3.7). Interestingly, 0.02% TMS-induced reduction in FluoVolt™ signal is greater than that induced by 0.0001% TTX (Figure 2.3.7). These findings suggest that Na_v blockers bind to neural plate cell Na_v and diminish inward Na^+ current, resulting in a hyperpolarized membrane. Na_v blockers altering Na^+ flow demonstrates that Na_v is functional and essential to neural plate cell resting membrane potential.

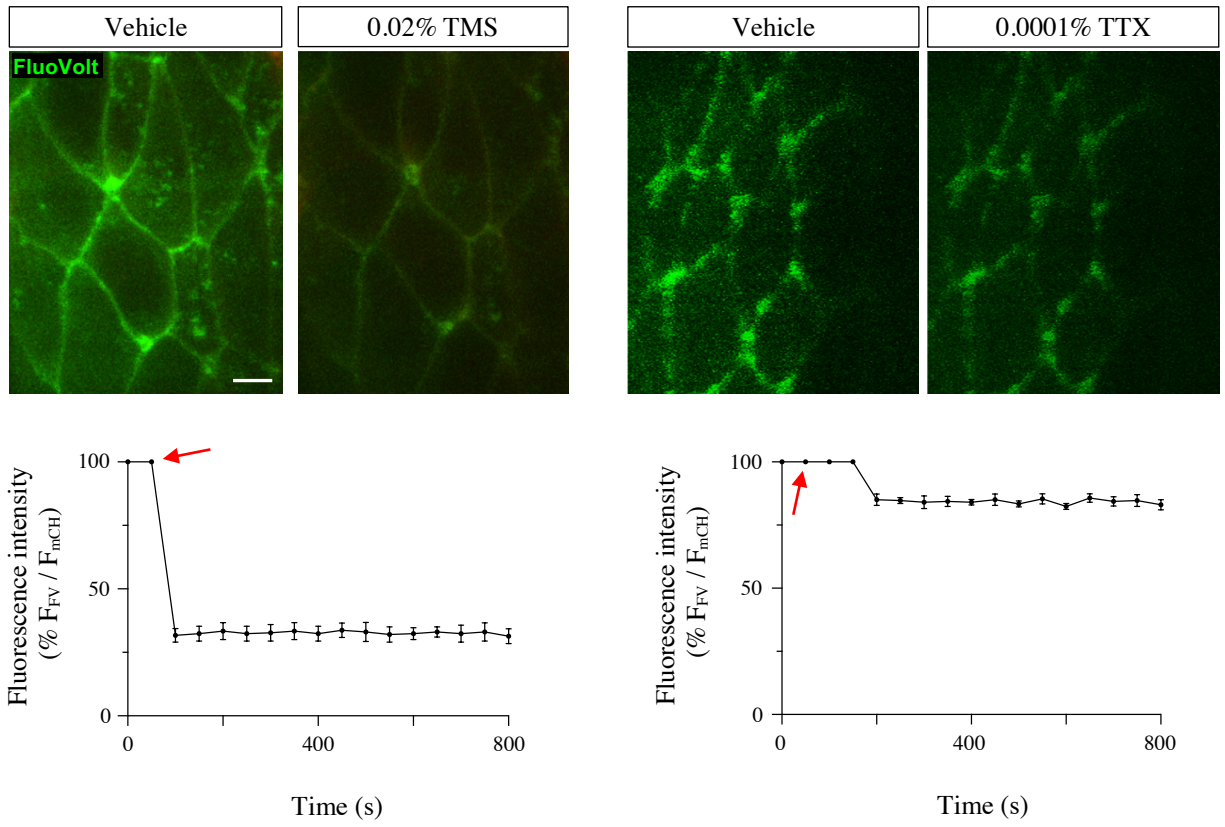

Figure 2.3.7. Na_v blockers hyperpolarize neural plate cells. Neural plate stage embryos (stage 15 to 17) expressing mCherry-Mem were incubated with the voltage-sensitive dye FluoVolt™. Embryos were time-lapse imaged with an acquisition rate of 0.1 Hz before and after the addition of 0.02% TMS or 0.0001% tetrodotoxin. Shown are representative images of neural plate before and after the addition of indicated solutions, scale bar 10 μm. Traces represent the mean $\pm$SEM percent change in FluoVolt / mCherry-Mem ratio over time, n > 6, red arrow shows the addition of the indicated solution.

2.4 Discussion

This study demonstrates the expression and localization of Na_v during neural plate folding and neural tube development in *Xenopus laevis* embryos. Scn1a transcripts appear in early neural plate *Xenopus laevis* embryos with transcript levels increasing as neural plate folding progresses (Sessions et al., 2016). I demonstrate the presence of Na_v protein throughout neurulation, with an apparent "shuttling period" suggested by Na_v expressed in

the cytosol in early neural plate stages with membrane localization as neural plate folding progresses (Figure 2.3.1). In the mature nervous system, Na_v are responsible for the depolarization of the neuronal cell membrane during the upstroke of an action potential. Na_v are essential for the propagation of action potentials, therefore they are enriched in strategic regions of the axonal membrane (Catterall et al., 2017). They are comprised of a single α-subunit that is arranged into four homologous domains (I-IV) each consisting of six transmembrane segments (S1-S6) (Catterall & Swanson, 2015). The voltage sensor of the channel is credited to the charged amino acids of the S4 segments of each domain. In the central nervous system the α-subunit is associated with two β-subunits which can influence channel gating and kinetics (Hull & Isom, 2018). The Na_v pore is divided into two parts: the outer mouth of the pore which is the site of ion selectivity and the inner cytoplasmic pore which serves as the activation gate (O'Leary & Chahine, 2017). The inner cytoplasmic pore is lined with the S6 segments and is the most common site of drug binding (Brodie, 2017; Sills & Rogawski, 2020). Because of their importance to the conduction of signals, Na_v are the target of a wide variety of local anesthetic, antidepressant, and antiepileptic drugs (O'Leary & Chahine, 2017).

The expression and localization of Na_v during *Xenopus laevis* neurulation highlights the fact that targeting Na_v during neural plate folding and neural tube formation may be a contributing mechanism underlying drug teratogenicity. This study demonstrates that Na_v blockers alter neural activity in the neural plate by affecting the resting membrane potential of neural plate cells and their Ca^{2+} dynamics. Both TMS and TTX reduce the Ca^{2+} activity of *Xenopus laevis* neural plate cells and reverse the characteristic developmental increase in Ca^{2+} dynamics during neural plate folding (Figure 2.3.4). The medial

neuroectoderm of *Xenopus laevis* exhibits spontaneous transients in intracellular calcium concentration, and these transients increase in frequency with the progression of neural plate folding (Sequerra et al., 2018). The AED valproic acid causes a similar reduction in neural plate cell Ca^{2+} activity resulting in neural tube defects (Sequerra et al., 2018). Noteworthy, the neural tube defects caused by valproic acid inhibition of Ca^{2+} activity can be rescued by enhancing ERK 1/2 activation, suggesting the importance of Ca^{2+}-mediated downstream signaling to neural plate folding (Sequerra et al., 2018). Calcium signaling has been shown to be required to activate neural fate by triggering neural-specific gene expression (Moreau et al., 2008). In addition, Ca^{2+} dynamics regulate actin contractions necessary for apical constriction in the folding neural plate (Christodoulou & Skourides, 2015) and regulate the expression of cell adhesion molecules responsible for the fusion of neural folds (Abdul-Wajid et al., 2015). I demonstrate that exposing neural plate stage embryos to Na_v blockers inhibits Ca^{2+} dynamics and results in neural tube defects (Figure 2.3.2).

While ion conductance is the basis of neurotransmission in the mature nervous system, the influence of ion currents and resting membrane potential during neurulation is still unclear. It has been shown that ion currents and membrane potential mediate cell division and cell cycle progression during early embryogenesis (Deng et al., 2007; Perathoner et al., 2014; Urrego et al., 2014). Sodium current is essential to neural differentiation (Messenger & Warner, 1979; Pai et al., 2015; Robinson & Stump, 1984). Neural plate stage *Xenopus laevis* embryos exposed to strophanthidin, a Na^+/K^+ ATPase inhibitor, display a reduction in neural differentiation and ultimately a 50% reduction in white matter of the mature nervous system (Messenger & Warner, 1979). The folding

neural plate of *Xenopus laevis* presents a current pattern consisting of Na^+-dependent inward current stronger in the mid-lateral neural plate which decreases near the midline of the neural groove (Robinson & Stump, 1984). Furthermore, spontaneous alterations in the resting membrane potential of axolotl neural plate cells during mid-neural plate stages have been shown to be mediated in part by Na^+/K^+ ATPase activity (Blackshaw & Warner, 1975).

I demonstrate that *Xenopus laevis* neural plate cells are hyperpolarized when exposed to Na_v blockers, suggesting that Na_v is an essential and functional participant of Na^+ flux during neural plate folding (Figure 2.3.7). Interestingly, I find that the resting membrane potential of neural plate cells throughout neurulation is dependent on K^+, Na^+, and Cl^- gradients (Figure 2.3.6). The resting membrane potential of mature neurons is governed by K^+ leaky channels but during neural plate stages I find that neural plate cells are depolarized by increasing extracellular K^+ of Na^+ (Figure 2.3.6), and hyperpolarized by Na_v blockers, suggesting that Na_v contributes to Na^+ permeability even at resting conditions.

Potential hypotheses to explain neural plate stage Na_v permeability to Na^+ at rest include; (1) Na_v at neural plate stages differs in structure and gating kinetics compared to mature Na_v or, (2) neural plate cells have a more depolarized resting membrane potential allowing for a high probability that Na_v remains in an open state. An example of a receptor that has a fetal- and adult-type subunit is the nicotinic acetylcholine receptors (AChRs) and studies have elucidated that the subunits differ in function and kinetics (Nayak et al., 2016). While the binding sites of fetal- and adult-AChRs have homology in the core amino acids, the fetal subunit has a 30-fold higher affinity to bind the neurotransmitter ACh (Nayak et

al., 2016). Moreover, Blackshaw & Warner demonstrated a spontaneous shift in the resting membrane potential of axolotl neural plate cells from depolarized to hyperpolarized, as well as changes in the establishment of ionic gradients (Blackshaw & Warner, 1975). Further studies to explore potential structural and functional characteristics of embryonic Na_v, as well as the resting membrane potential and ionic currents during neural plate folding and neural tube formation is essential to further understand the role of Na_v in these processes and how interfering with their embryonic function can be avoided in newly developed drugs and therapeutics.

Chapter III
Voltage-gated sodium channel-targeting antiepileptic drugs affect neural activity during neurulation

3.1 Introduction

3.1.1 Mechanisms of antiepileptic drug action

Antiepileptic drugs (AEDs) decrease pathological hyperexcitability of the cerebral cortex via a multitude of primary targets and mechanisms of action (Falco-Walter, 2020; Kellogg & Meador, 2017). AEDs are categorized by their primary actions at various molecular targets, including (1) enhancement of γ-aminobutyric acid (GABA)-mediated inhibition, (2) inhibition of synaptic excitation mediated by ionotropic glutamate receptors, (3) modulation of voltage-gated ion channels (Davies, 1995; Kellogg & Meador, 2017; Rogawski et al., 2016; Sankaranen & Lachhwani, 2015). Noteworthy, AEDs achieve therapeutic benefits by targeting multiple cellular mechanisms, likely improving efficacy and tolerability (Rogawski et al., 2016; Rogawski & Loscher, 2004). The mechanism of action of several AEDs, including valproic acid and levetiracetam, remain unclear despite decades of clinical use (Loscher et al., 2002). AEDs can strategically target the enhancement of inhibitory (GABA) neurotransmission or the attenuation of excitatory (glutamate) neurotransmission to control the imbalance of the epileptic cerebral cortex (Sankaranen & Lachhwani, 2015). Phenobarbital and benzodiazepines bind to the GABA-A receptor complex increasing the overall probability that the chloride channel is open (Davies, 1995; Rogawski & Loscher, 2004).

Blockade of voltage-gated sodium channels (Na_v) is the most common mechanism of action among currently available AEDs. Despite structural differences, there is a common binding site for Na_v-AEDs on the α-subunit of Na_v in the inner pore region of

domain IV transmembrane segment S6 (Kuo et al., 1998). Na_v cycle through three conformational states; (1) closed state at hyperpolarized potentials, (2) open state that is permeable to Na^+ at depolarized potentials, and (3) non-conducting inactivated state following depolarization (Catterall, 1992; 2017). Na_v-AEDs bind with preferential affinity for Na_v in the inactivated state (Schwarz & Grigat, 1989), which slows the conformational recycling process and delays the recovery of the channel. Therefore, Na_v -AEDs extend the 'refractory' period and reduce the conductance of Na_v, resulting in an inhibition of repetitive neuronal firing (MacDonald & Kelly, 1995). Na_v-AEDs, including carbamazepine (CBZ) and lamotrigine (LTG), block high-frequency repetitive spike firing that is necessary to spread seizure activity without affecting ordinary neural activity (Rogawski & Loscher, 2004).

3.1.2 Proposed mechanisms of antiepileptic drug teratogenicity

Several hypotheses have been set forward to elucidate the mechanisms by which AEDs disrupt embryonic development. The prevailing paradigm is that AED-induced NTDs occur via off-target effects, including (1) inhibition of folate metabolism (Finnell et al., 2003; Wegner & Nau, 1992) (2) buildup of AED metabolites and oxidative stress (Finnell et al., 1995; Morimoto et al., 2016; Pippenger, 2003) and (3) inhibition of histone deacetylases altering gene expression and inhibiting cell proliferation necessary during rapid growth (Eyal et al., 2004; Gurvich et al., 2005).

Studies in mice have shown that CBZ is biotransformed to a reactive teratogenic metabolite (Finnell et al., 1995). The primary metabolism pathway of CBZ involves the oxidative formation of CBZ-10, 11-epoxide (Lindhout et al., 1984). When pregnant mice were treated with this metabolite, it increased the incidence of malformations in fetuses

(Tecoma, 1999). Valproic acid (VPA) is a first-generation AED with a 6.2% absolute risk of major congenital malformations, threefold the risk of CBZ (Harden, 2008). Therefore, VPA is most often used in studies attempting to elucidate the mechanisms of AED teratogenicity. VPA has been shown to act as a histone deacetylase (HDAC) inhibitor (Finnell et al., 2002; Phiel et al., 2001; Gottlicher et al., 2001). Modulating the acetylation status of histones can inhibit cell growth and induce terminal differentiation, adversely altering the typical pattern of embryonic development (Martin & Regan, 1991). Studies in rats have shown that VPA provoked hepatic DNA hypomethylation that impairs methionine availability and induces DNA hypomethylation (Alonso-Aperte et al., 1999). In addition, VPA interference with embryonic folate metabolism is a contributing mechanism to VPA-induced neural tube defects in mice (Wegner & Nau, 1992). VPA in murine embryos alters the pattern of folate metabolites resulting in neural tube defects. In contrast, a closely related analog of VPA does not alter folate metabolites or lead to neural tube defects (Wegner & Nau, 1992).

3.1.3 Evidence of antiepileptic drugs targeting neural activity in early stages of neurodevelopment

It is thought that AED efficiency and tolerability in the mature nervous system are likely due to AED action at multiple cellular targets (Hill et al., 2010; Ikonomidou & Turski, 2010; Macdonald & Kelly, 1995). VPA has been proposed to interfere with glutamate signaling by specifically inhibiting NMDA receptor-mediated synaptic activity (Gean et al., 1994; Gobbi & Janiri, 2006; Ko et al., 1997; Martin & Pozo, 2004; Zeise et al., 1991). Recent studies have demonstrated that VPA inhibits glutamate signaling in *Xenopus laevis* neural plate stage embryos, similarly to the glutamate antagonist D-AP5, and induces neural tube defects (Sequerra et al., 2018). These findings suggest that a

contributing mechanism of VPA teratogenesis is the disruption of NMDA receptor-mediated signaling in neural plate cells of the developing embryo (Sequerra et al., 2018). VPA has been shown to cause an increase in rat neuronal progenitors (Laeng et al., 2004) and *Xenopus laevis* neural plate cells (Sequerra et al., 2018). These findings challenge the proposed explanation of VPA HDAC inhibitor action underlying teratogenesis, as inhibition of HDACs would decrease cell proliferation. In addition, VPA exposure reduces *Xenopus laevis* neural plate cell calcium activity and results in neural tube defects (Sequerra et al., 2018). Interestingly, the partial rescue of calcium signaling, and ultimately neural tube defects, can be achieved with NMDA treatment of the embryos (Sequerra et al., 2018). As we continue to advance our understanding of neural activity during neural plate folding and neural tube development, it is necessary to explore the potential of AED action at their primary targets as an underlying contributor to their teratogenic risk.

In this final chapter, I test the hypothesis that voltage-gated sodium channel-targeting AEDs (Na_v-AEDs) disrupt neural activity essential for neural tube formation in *Xenopus laevis* embryos. I discover the action of Na_v-AEDs on neural plate cell calcium dynamics and resting membrane potential in *Xenopus laevis* embryos.

3.2 Materials and Methods

3.2.1 Animals

Mature oocytes were collected from *Xenopus laevis* females previously injected with human chorionic gonadotropin hormone. *In vitro* fertilization was performed by exposing the oocytes to a small piece of minced testis in a dish with 10% Marc's Modified Ringers

(MMR) saline solution containing (mM): 10 NaCl, 0.2 KCl, 0.1 $MgSO_4$, 0.5 HEPES, 5 EDTA, and 0.2 $CaCl_2$. This defined time 0 of fertilization. Fertilized embryo jelly coats were partially removed by incubation with 2% cysteine solution (pH 8) followed by 10% MMR washes. Embryos were grown in 10% MMR at 23ºC. Animals were handled under an approved Institutional Animal Care and Use Committee protocol and guidelines.

3.2.2 Calcium imaging in the presence of antiepileptic drugs

Two- to four-cell stage *Xenopus laevis* embryos were injected with GCaMP6s mRNA (0.8 – 1 ng per embryo). GCaMP6s mRNA was prepared as described in chapter 2 (section 2.2.6). Embryos were incubated with 6% Ficoll in 10% MMR for 1-hour post-injection and grown to neural plate stages in saline (10% MMR). Neural plate stage embryos 16 – 19 hours postfertilization (hpf) were imaged using a Sweptfield confocal microscope (Nikon) at an acquisition rate of 0.1 Hz for 35 min. Embryos were imaged for a control period (0-5 min) and a treatment period (5-35 min). A single embryo was situated for dorsal midline imaging using clay in an imaging dish with saline (10% MMR). Following the 5 min control period, CBZ or LTG stock solutions were added to the imaging dish to achieve the desired treatment concentration (0.1 or 1 mM AED in 0.05% DMSO, n = 12). Controls included the addition of (1) saline (10% MMR; n = 12) or (2) DMSO for a final imaging concentration of 0.05% (n = 30). Stock solutions were made so that the volume (250 μL) added to the imaging dish was constant across groups. As in previous studies, calcium transients were detected by a peak change in fluorescence of at least twice the level of the noise (Belgacem and Borodinsky, 2011; Borodinsky et al., 2004; Borodinsky and Spitzer, 2007; Sequerra et al., 2018; Swapna and Borodinsky, 2012; Tu and Borodinsky, 2014; (Figure 2.3.1)). Calcium transients were quantified at various time points (0-5, 5-10, and

30-35 minutes). The number of calcium transients for each treatment period was compared to the control period to assess the percent change in calcium transients over time. Significance was determined by one-way ANOVA followed by Tukey's multiple comparisons test.

3.2.3 Membrane potential sensor incubation

Xenopus laevis embryo jelly coats were partially removed by incubation with 2% cysteine solution (pH 8) followed by saline (10% MMR) washes. Two-cell stage embryos (1.5 hpf) were injected with membrane mCherry (mCherry-Mem) was a gift from Narasimhan Gautam (Addgene plasmid #36075; http://n2t.net/addgene:36075; RRID: Addgene_36075) (Chisari et al., 2009). Embryos were incubated with 6% Ficoll in 10% MMR for 1-hour post-injection and grown to neural plate stages in saline (10% MMR). When embryos reached stage 13 - 14 (15 – 16 hpf), they were loaded with FluoVolt™ Membrane Potential dye (FluoVolt™ Membrane Potential Kit, catalog # F10488, ThermoFisher) using a 1:10 solution of FluoVolt dye (488) to Powerload Concentrate Loading Buffer with probenecid (catalog # P36400, ThermoFisher). Embryos were incubated with the FluoVolt™ solution for 30 min, protected from light at 23ºC. Embryos were subsequently washed three times with saline (10% MMR) and maintained at 23ºC (Figure 2.3.5).

3.2.4 Imaging of membrane potential in the presence of antiepileptic drugs

Xenopus laevis neural plate stage embryos (16 – 19 hpf) previously loaded with FluoVolt™ Membrane Potential Dye were imaged using a Sweptfield confocal microscope (Nikon) at an acquisition rate of 0.1 Hz for 15 min. A single embryo was situated for dorsal midline imaging using clay in an imaging dish with saline (10% MMR). Embryos were imaged for

a control period (0-5 min) and a treatment period (5-15 min). Following the 5 min control period, stock solutions of CBZ or LTG were added (250 μL) to the imaging solution to achieve a final concentration of 500 μM AED in 0.05% DMSO (N > 3, n > 5 per group). Controls included the addition of (1) saline (10% MMR; N > 3, n > 5) and (2) DMSO for a final imaging concentration of 0.05% (N > 3, n > 5). The percent change in fluorescence intensity (AU) over time of FluoVolt™ was normalized using the mCherry-Mem fluorescence intensity (Figure 2.3.5). The data are reported as the mean±SEM percent change in FluoVolt™ over mCherry-Mem ratio (N > 3, n > 5).

3.2.5 Statistical analysis

ANOVA evaluated significance, followed by Tukey's post hoc multiple comparisons test. N ≥ 3 independent fertilizations and n ≥ 6 embryos per group for all data sets. Differences were considered significant when $p<0.05$.

3.3 Results

3.3.1 Antiepileptic drugs reverse the developmental progression of calcium dynamics of neural plate cells during neurulation mimicking the effect of Na_v blockers

Xenopus laevis embryos exposed to either of the Na_v-AEDs, CBZ or LTG during neurulation resulted in diminished neural plate cell calcium dynamics detected by the genetically-encoded calcium sensor GCaMP6s (Figure 3.3.1). I find that 1 mM CBZ reduces the frequency of Ca^{2+} transients within 5 min of incubation and this decrease becomes even stronger after 30 min of exposure (Figure 3.3.1). Interestingly, 1 mM LTG resulted in a faster reduction in Ca^{2+} transient frequency in neural plate cells than CBZ (Figure 3.3.1). Lower (0.1 mM) dose Na_v-AEDs were slower and less potent at eliciting a significant reduction in Ca^{2+} transient frequency in the folding neural plate (Figure 3.3.1).

Comparing the effect of Na_v-AEDs on Ca^{2+} dynamics in the neural plate to the significant increase in Ca^{2+} dynamics that embryos exhibit in a 30-min period of neural plate folding demonstrates that these drugs reverse the normal developmental progression of Ca^{2+} activity during neural tube formation (Figure 3.3.1). Moreover, this reversal effect of AEDs on developmentally-regulated Ca^{2+} dynamics is similar to the effect of Na_v blockers, suggesting that CBZ and LTG may inhibit Ca^{2+} transients by impairing Na_v function.

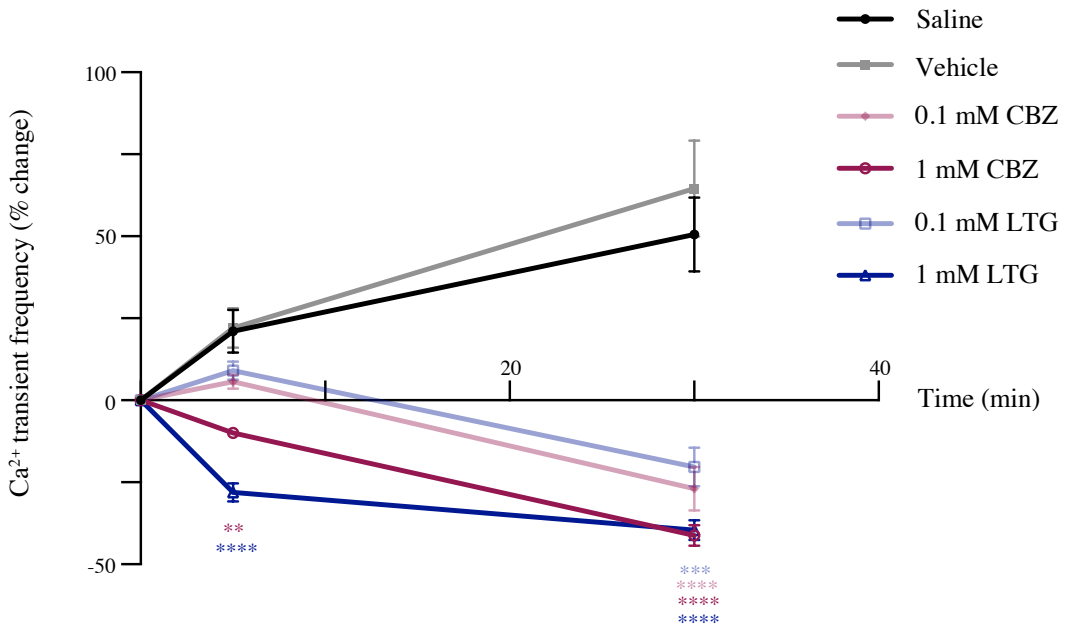

Figure 3.3.1. AEDs reverse the developmental progression of Ca^{2+} dynamics of neural plate cells during neurulation. Ca^{2+} transients were detected by time-lapse *in vivo* imaging whole embryos (stage 15, 17.5 hpf) expressing the GCaMP6s Ca^{2+} sensor. Embryos were incubated in either saline (n = 12), vehicle (0.05% DMSO, n = 30), LTG (0.1 or 1 mM, n = 12) or CBZ (0.1 or 1 mM, n = 12). Percent change was calculated by comparing the number of transients detected 5 min before starting the experiment (in saline for all groups) to the number of transients detected at both 5 min and 30 min following the addition of the treatment (or control). N ≥ 6 independent experiments, mean±SEM, **p<0.01, ***p<0.001, ****p<0.0001, one-way ANOVA followed by Tukey's multiple comparisons test to compare vehicle to treatment groups.

3.3.2 Antiepileptic drugs hyperpolarize neural plate cells mimicking the effect of Na_v blockers

FluoVolt™ membrane potential dye is a useful reporter for studying the effects of ions and pharmacological agents on neural plate cell resting membrane potential during *Xenopus laevis* neural tube development. It is advantageous over other membrane potential probes because it is easy to use, gentle on the sample, and compatible with standard imaging equipment (see section 2.3.5). Embryos were injected with mCherry-Mem as a control for membrane movement inherent to neural plate folding. The mCherry-Mem-expressing embryos were loaded with FluoVolt™ and exposed to AEDs during live confocal imaging to assess the change in fluorescence, indicating a change in resting membrane potential. An increase in fluorescence intensity indicates depolarization of the membrane, while a decrease is indicative of a hyperpolarized membrane (see sections 2.3.5 and 2.3.6). Time-lapse imaging with FluoVolt™ reveals that exposure to 500 μM CBZ or LTG reduces the voltage-sensor fluorescence intensity (Figure 3.3.2). The change elicited by CBZ was faster than that of LTG which could be explained by potential differences in the AED's ability to penetrate the embryo jelly coat (Figure 3.3.2). These results provide evidence that AEDs hyperpolarize neural plate cells during neurulation, similarly to the action elicited by Na_v-blockers (Figures 2.3.7; 3.3.2).

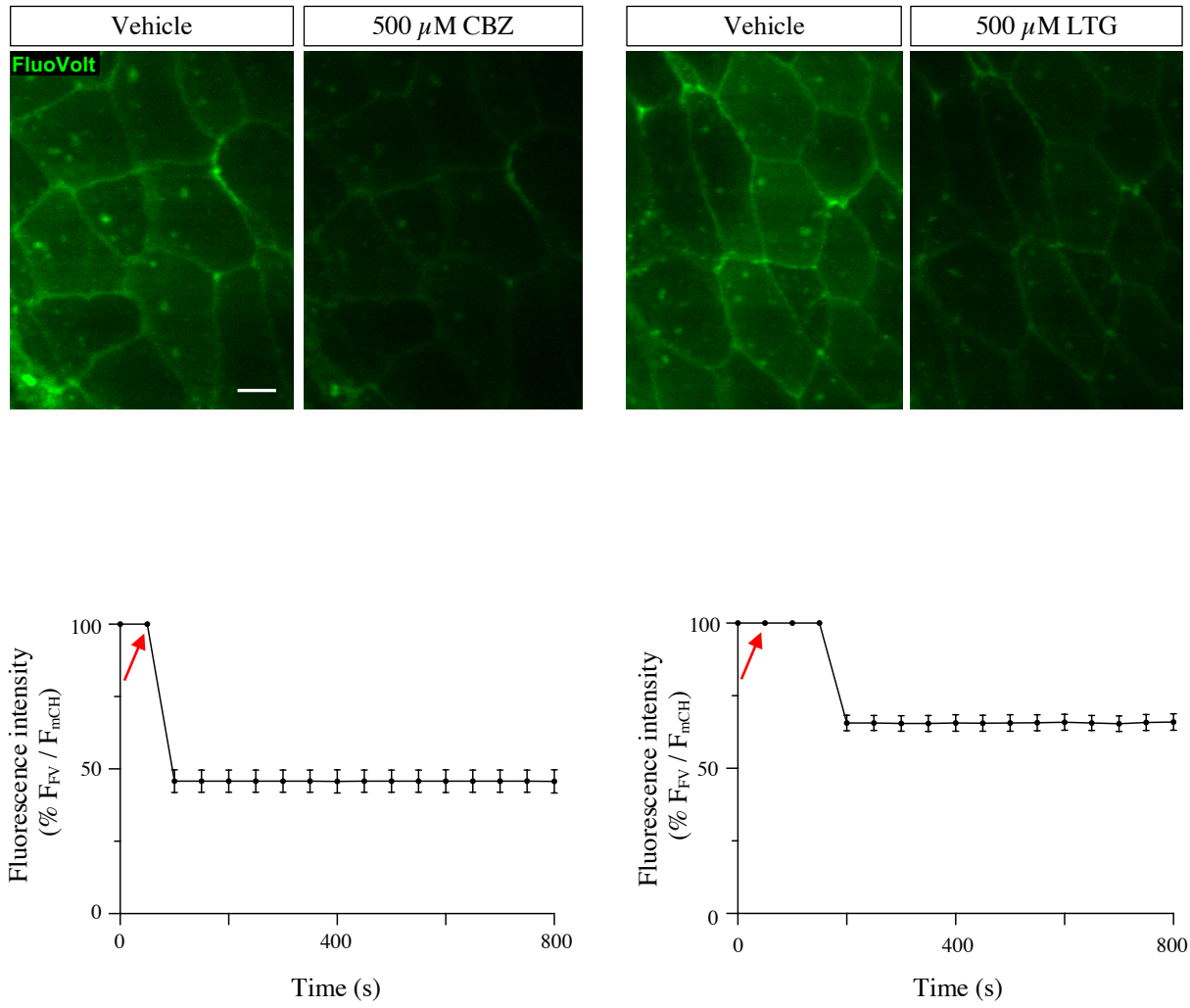

Figure 3.3.2. AEDs hyperpolarize neural plate cells. Neural plate stage embryos (stage 15 to 17) expressing mCherry-Mem were incubated with the voltage-sensitive dye FluoVolt™. Embryos were time-lapse imaged with an acquisition rate of 0.1 Hz before and after the addition of 500 μM CBZ or LTG. Shown are representative images of neural plate before and after the addition of indicated solutions, scale bar 10 μm. Traces represent the mean ±SEM percent change in FluoVolt (FV) / mCherry-Mem (mCH) ratio over time; $N \geq 3$, $n \geq 5$; red arrow shows the addition of the indicated solution.

3.4 Discussion

While the risk of some AEDs has been established, the mechanisms underlying teratogenicity are still under debate. In addition, newer and highly prescribed AEDs have unknown teratogenic potential. LTG is a new generation Na_v-AED that is thought to inhibit glutamate release by action at Na_v (Leach et al., 1986). While its molecular makeup is dissimilar to CBZ, the drugs bind to the Nav pore at a common binding site on the α-subunit in the inner pore region of domain IV transmembrane segment S6 (Kuo et al., 1998). The similar Na_v binding affinity and kinetics of CBZ and LTG pose speculation as to the accurate safety profile of LTG for use in pregnancy.

This study provides evidence that both CBZ and LTG alter neural activity in the neural plate by affecting the resting membrane potential of neural plate cells and their calcium dynamics. The medial neuroectoderm of *Xenopus laevis* exhibits spontaneous transients in intracellular calcium concentration, and these transients increase in frequency with the progression of neural plate folding (Sequerra et al., 2018). Calcium signaling is required to activate neural fate (Moreau et al., 2008). Progressive calcium signaling has been shown to regulate actin contractions necessary for apical constriction in the folding neural plate (Christodoulou & Skourides, 2015) and regulate the expression of cell adhesion molecules responsible for the fusion of neural folds (Abdul-Wajid et al., 2015). When neural plate stage *Xenopus laevis* embryos are exposed to clinically relevant concentrations of Na_v-AEDs, there is a reduction and reversal of the characteristic developmental increase in calcium activity during neural plate folding (Figure 3.3.1). Similarly, previous studies have shown that VPA diminishes calcium activity in *Xenopus laevis* neural plate cells, resulting in neural tube defects (Sequerra et al., 2018).

Xenopus laevis neural plate cell resting membrane potential is hyperpolarized by exposure to either CBZ or LTG (Figure 3.3.2). Classic studies have shown the relevance of sodium currents and resting membrane potential during neural plate stages (Blackshaw & Warner, 1975; Messenger & Warner, 1979; Robinson & Stump, 1984). In mid-neural plate stage axolotl embryos, a spontaneous increase in resting membrane potential occurs and an increase in extracellular potassium during this change causes neural plate cells to hyperpolarize (Blackshaw & Warner, 1975). The spontaneous increase in resting membrane potential and the potassium-induced hyperpolarization of neural plate cells can be prevented by the addition of cardiac glycosides, suggesting that the sodium pump is functional following neural induction (Blackshaw & Warner, 1975). Sodium current is essential to neural differentiation (Messenger & Warner, 1979; Pai et al., 2015; Robinson & Stump, 1984), and when neural plate stage *Xenopus laevis* embryos are exposed to a Na^+/K^+ATPase inhibitor, there is a reduction in neural differentiation and white matter of the mature nervous system (Messenger & Warner, 1979). I observed a dose-dependent increase in the number of neural plate cells in Na_v-AED exposed *Xenopus laevis* embryos (Figure 1.3.3). In addition, the ratio of Sox2+ neural progenitor cells is increased in embryos exposed to higher doses of Na_v-AEDs, suggesting that Na_v blockade decreased differentiation and preserved the "stemness" phenotype (Figure 1.3.3).

Most studies attribute AED's increased risk of NTDs to the off-target effects of these drugs (Eyal et al., 2004; Finnell et al., 2003; Gurvich et al., 2005; Morimoto et al., 2016; Pippenger, 2003; Wegner & Nau, 1992). However, my findings suggest that a contributing mechanism of Na_v-AED teratogenicity is the disruption of embryonic neural cell excitability via interactions with embryonic Na_v causing an increase in neural plate cell

proliferation and NTDs. This study supports growing evidence that neural activity is critical to the early stages of embryogenesis (Borodinsky and Spitzer, 2006, 2007; Goyal et al., 2020; Kapur et al., 1991; Lauder et al., 1981; Root et al., 2008; Rowe et al., 1993; Sequerra et al., 2018; Smith & Walsh, 2020) and the use of drugs that antagonize essential components of embryonic excitability will result in NTDs. Therefore, the avoidance of Na_v or the exploitation of potential differences between embryonic and mature Na_v to develop new AEDs would minimize the risk of AED-induced NTDs.

3.5 Conclusions & Future Perspectives

This work demonstrates that Na_v is expressed by *Xenopus laevis* neural plate cells throughout neural plate folding and neural tube closure and its insertion in neural plate cell membranes increases with the progression of neural tube formation. These findings suggest that Na_v may play an important role in this process. Importantly, both Na_v blockers and Na_v-AEDs elicit neural tube defects when exposed to neurulating *Xenopus laevis* embryos. AED exposure increased the overall number of cells in the neural tube, with higher doses increasing the number of neural progenitor cells, suggesting that AEDs diminish neural differentiation (Figure 3.5.1). In addition, Na_v blockers and Na_v-AEDs comparably reduce neural plate cell calcium activity and reverse the developmental progression of neural plate cell calcium dynamics during neurulation suggesting that AEDs may inhibit calcium transients by impairing Na_v function (Figure 3.5.1).

Moreover, this study establishes FluoVolt™ membrane potential dye as a useful probe for studying neural plate cell resting membrane potential in *Xenopus laevis* embryos and that the resting membrane potential of neural plate cells is dependent on K^+, Na^+, and

Cl^- gradients. Na_v blockers and Na_v-AEDs cause neural plate cells to hyperpolarize. This noteworthy finding of neural cell resting membrane potential dependence on Na^+ poses speculation as to how Na_v is open and permeable to Na^+ at rest. Here I propose that the increased probability that Na_v is open and permeable to Na^+ at rest is due to either (1) structural differences in embryonic Na_v or, (2) neural plate cells are more depolarized at rest. Regardless of the gating mechanism, the findings of this study propose a model of neural tube formation where spontaneous activation of Na_v leads to further depolarization of neural plate cells and activation of NMDAR and calcium dynamics. This calcium activity is important for regulating the neural plate cell cycle and neural tube formation. Na_v-AEDs interfere with Na^+ currents and calcium dynamics leading to neural tube defects.

The evidence of Na_v expression, localization, and function during neural plate folding and neural tube formation highlights the need for future studies to further characterize embryonic Na_v in an attempt to identify preventative therapeutic measures to reduce the risk of NTDs associated with Na_v-AEDs.

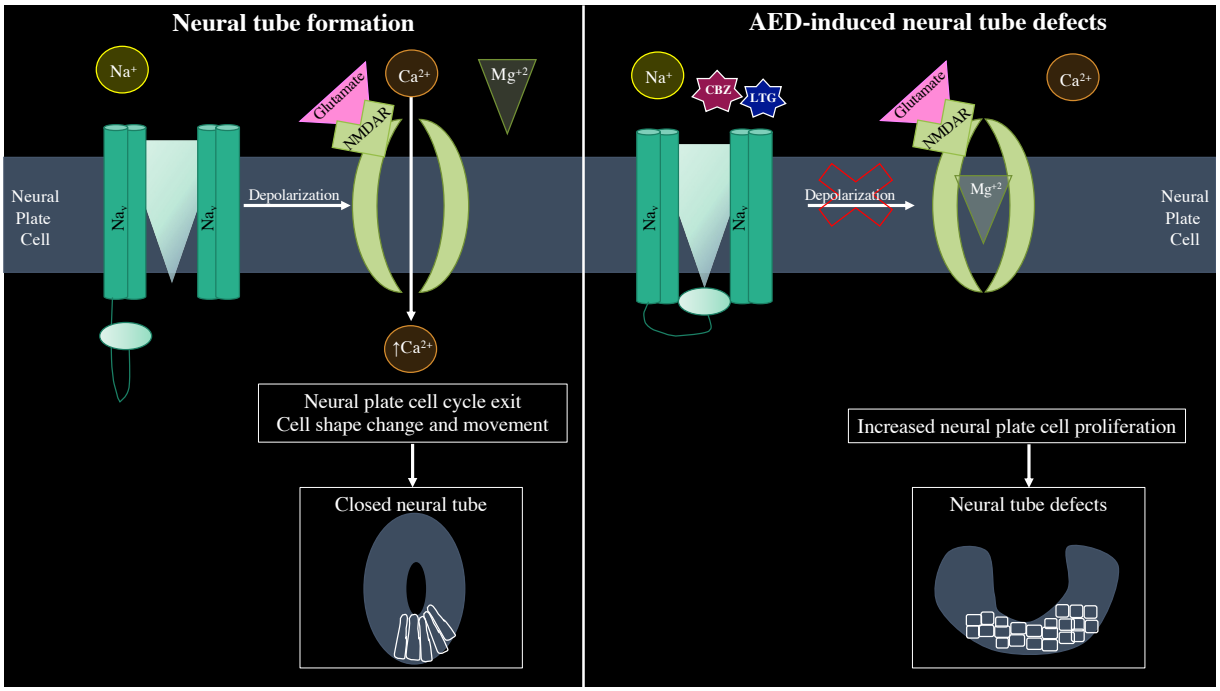

Figure 3.5.1. Model of mechanisms of Na_v-antiepileptics induced neural tube defects. Resting membrane potential of neural plate cells allows for spontaneous activation of Na_v which in turn leads to further depolarization of neural plate cells and activation of NMDAR and calcium dynamics. This calcium activity is important for regulating neural plate cell cycle and neural tube formation. Na_v-AEDs interfere with Na^+ currents and calcium dynamics leading to neural tube defects.

REFERENCES

Abdul-Wajid, S., Morales-Diaz, H., Khairallah, S.M., and Smith, W.C. (2015). T-type Calcium Channel Regulation of Neural Tube Closure and EphrinA/EPHA Expression. Cell Rep 13, 829-839.

Aiken, J., Buscaglia, G., Bates, E. A., & Moore, J. K. (2017). The α-Tubulin gene TUBA1A in Brain Development: A Key Ingredient in the Neuronal Isotype Blend. Journal of developmental biology, 5(3), 8.

Alonso-Aperte E, Ubeda N, Achon M, Perez-Miguelsanz J, Varela-Moreiras G. Impaired methionine synthesis and hypomethylation in rats exposed to valproate during gestation. Neurology. 1999;52(4):750–756.

Arfman IJ, Wammes-van der Heijden EA, Ter Horst PGJ, Lambrechts DA, Wegner I, Touw DJ. Therapeutic Drug Monitoring of Antiepileptic Drugs in Women with Epilepsy Before, During, and After Pregnancy. Clin Pharmacokinet. 2020 Apr;59(4):427-445. doi: 10.1007/s40262-019-00845-2. PMID: 31912315.

Balashova OA, Visina O, Borodinsky LN. Folate receptor 1 is necessary for neural plate cell apical constriction during Xenopus neural tube formation. Development. 2017 Apr 15;144(8):1518-1530. doi: 10.1242/dev.137315. Epub 2017 Mar 2. PMID: 28255006; PMCID: PMC5399658.

Bangar S, Shastri A, El-Sayeh H, Cavanna AE. Women with epilepsy: clinically relevant issues. Funct Neurol. 2016;31(3):127-134. doi:10.11138/fneur/2016.31.3.127

Battino, D., Binelli, S., Caccamo, M.L., Canevini, M.P., Canger, R., Como, M.L., Croci, D., De Giambattista, M., Granata, T., Pardi, G., et al. (1992a). Malformations in offspring of 305 epileptic women: a prospective study. Acta Neurol Scand 85, 204-207.

Battino, D., Granata, T., Binelli, S., Caccamo, M.L., Canevini, M.P., Canger, R., Croci, D., Fumarola, C., Mai, R., Molteni, F., et al. (1992b). Intrauterine growth in the offspring of epileptic mothers. Acta Neurol Scand 86, 555-557.

Belgacem, Y.H., and Borodinsky, L.N. (2011). Sonic hedgehog signaling is decoded by calcium spike activity in the developing spinal cord. Proc Natl Acad Sci U S A 108, 4482-4487.

Belgacem, Y.H., and Borodinsky, L.N. (2015). Inversion of Sonic hedgehog action on its canonical pathway by electrical activity. Proc Natl Acad Sci U S A 112, 4140-4145.

Belgacem YH, Hamilton AM, Shim S, Spencer KA, Borodinsky LN. The Many Hats of Sonic Hedgehog Signaling in Nervous System Development and Disease. J Dev Biol. 2016 Dec 10;4(4):35. doi: 10.3390/jdb4040035. PMID: 29615598; PMCID: PMC5831807.

Berry RJ, Li Z, Erickson JD, Li S, Moore CA, Wang H, Mulinare J, Zhao P, Wong LY, Gindler J, Hong SX, Correa A. Prevention of neural-tube defects with folic acid in China. China-U.S. Collaborative Project for Neural Tube Defect Prevention. N Engl J Med. 1999 Nov 11;341(20):1485-90. doi: 10.1056/NEJM199911113412001. Erratum in: N Engl J Med. 1999 Dec 9;341(24):1864. PMID: 10559448.

Blackshaw SE, Warner AE. Alterations in resting membrane properties during neural plate stages of development of the nervous system. J Physiol. 1976 Feb;255(1):231-47. doi: 10.1113/jphysiol.1976.sp011277. PMID: 1255516; PMCID: PMC1309242.

Blom, H.J., Shaw, G.M., den Heijer, M., and Finnell, R.H. (2006). Neural tube defects and folate: case far from closed. Nat Rev Neurosci 7, 724-731.

Borodinsky, L.N., Root, C.M., Cronin, J.A., Sann, S.B., Gu, X., and Spitzer, N.C. (2004). Activity-dependent homeostatic specification of transmitter expression in embryonic neurons. Nature 429, 523-530.

Borodinsky LN, Belgacem YH, Swapna I, Sequerra EB. Dynamic regulation of neurotransmitter specification: relevance to nervous system homeostasis. Neuropharmacology. 2014 Mar;78:75-80. doi: 10.1016/j.neuropharm.2012.12.005. Epub 2012 Dec 25. PMID: 23270605; PMCID: PMC3628948.

Borodinsky LN. (2017). Xenopus laevis as a Model Organism for the Study of Spinal Cord Formation, Development, Function and Regeneration. Front. Neural Circuits 11:90. doi: 10.3389/fncir.2017.00090

Borodinsky LN, Belgacem YH, Swapna I, Visina O, Balashova OA, Sequerra EB, Tu MK, Levin JB, Spencer KA, Castro PA, Hamilton AM, Shim S. Spatiotemporal integration of developmental cues in neural development. Dev Neurobiol. 2015 Apr;75(4):349-59. doi: 10.1002/dneu.22254. Epub 2014 Dec 10. PMID: 25484201; PMCID: PMC4363288.

Borodinsky, L.N., and Spitzer, N.C. (2006). Second messenger pas de deux: the coordinated dance between calcium and cAMP. Sci STKE 2006, pe22.

Borodinsky, L.N., and Spitzer, N.C. (2007). Activity-dependent neurotransmitter-receptor matching at the neuromuscular junction. Proc Natl Acad Sci U S A 104, 335-340.

Brodie MJ. Sodium Channel Blockers in the Treatment of Epilepsy. CNS Drugs. 2017 Jul;31(7):527-534. doi: 10.1007/s40263-017-0441-0. PMID: 28523600.

Catterall, W.A., 1992 Oct. Cellular and molecular biology of voltage-gated sodium channels. Physiol. Rev. 72 (4 Suppl. l), S15–S48.

Catterall, W.A., 2017 Sep. Forty years of sodium channels: structure, function, pharmacology, and epilepsy. Neurochem. Res. 42 (9), 2495–2504.

Catterall WA, Swanson TM. Structural Basis for Pharmacology of Voltage-Gated Sodium and Calcium Channels. Mol Pharmacol. 2015 Jul;88(1):141-50. doi: 10.1124/mol.114.097659. Epub 2015 Apr 6. PMID: 25848093; PMCID: PMC4468632.

Ceriani F, Mammano F. A rapid and sensitive assay of intercellular coupling by voltage imaging of gap junction networks. Cell Commun Signal. 2013 Oct 21;11:78. doi: 10.1186/1478-811X-11-78. PMID: 24144139; PMCID: PMC3819673.

Chen, T.W., Wardill, T.J., Sun, Y., Pulver, S.R., Renninger, S.L., Baohan, A., Schreiter, E.R., Kerr, R.A., Orger, M.B., Jayaraman, V., et al. (2013). Ultrasensitive fluorescent proteins for imaging neuronal activity. Nature 499, 295-300.

Christodoulou, N., and Skourides, P.A. (2015). Cell-Autonomous Ca(2+) Flashes Elicit Pulsed Contractions of an Apical Actin Network to Drive Apical Constriction during Neural Tube Closure. Cell Rep 13, 2189-2202.

Copp AJ, Greene NDE. Neural tube defects--disorders of neurulation and related embryonic processes. Wiley Interdiscip. Rev. Dev. Biol. 2013;2(2):213–27

Correa A, Botto L, Liu YC, Mulinare J, Erickson JD. Do multivitamin supplements attenuate the risk for diabetes-associated birth defects? Pediatrics. 2003;111:1146–51.

Cunnington M and Tennis P: International Lamotrigine Pregnancy Registry Scientific Advisory Committee: Lamotrigine and the risk of malformations in pregnancy. Neurology. 64:955–960. 2005.

Davidson L. A., Keller R. E. (1999). Neural tube closure in Xenopus laevis involves medial migration, directed protrusive activity, cell intercalation and convergent extension. Development 126, 4547–4556.

Davies JA. Mechanisms of action of antiepileptic drugs. Seizure. 1995 Dec;4(4):267-71. doi: 10.1016/s1059-1311(95)80003-4. PMID: 8719918.
Detrait, E.R., George, T.M., Etchevers, H.C., Gilbert, J.R., Vekemans, M., and Speer, M.C. (2005). Human neural tube defects: developmental biology, epidemiology, and genetics. Neurotoxicol Teratol 27, 515-524.
Edlund A. F., Davidson L. A., Keller R. E. (2013). Cell segregation, mixing, and tissue pattern in the spinal cord of the Xenopus laevis neurula. Dev. Dyn. 242, 1134–1146. 10.1002/dvdy.24004
Eyal S, Yagen B, Sobol E, Altschuler Y, Shmuel M, Bialer M. The activity of antiepileptic drugs as histone deacetylase inhibitors. Epilepsia. 2004 Jul;45(7):737-44. doi: 10.1111/j.0013-9580.2004.00104.x. PMID: 15230695.
Falco-Walter J. Epilepsy-Definition, Classification, Pathophysiology, and Epidemiology. Semin Neurol. 2020 Dec;40(6):617-623. doi: 10.1055/s-0040-1718719. Epub 2020 Nov 5. PMID: 33155183.
Finnell RH, Bennett GD, Slattery JT, Amore BM, Bajpai M, Levy RH. Effect of treatment with phenobarbital and stiripentol on carbamazepine-induced teratogenicity and reactive metabolite formation. Teratology 1995;52:324–332.
Finnell, R.H., Gould, A., and Spiegelstein, O. (2003). Pathobiology and genetics of neural tube defects. Epilepsia 44 Suppl 3, 14-23.
Forcelli PA, Janssen MJ, Vicini S, Gale K. Neonatal exposure to antiepileptic drugs disrupts striatal synaptic development. Ann Neurol2012;72:363–372.
Gean, P.W., Huang, C.C., Hung, C.R., and Tsai, J.J. (1994). Valproic acid suppresses the synaptic response mediated by the NMDA receptors in rat amygdalar slices. Brain Res Bull 33, 333-336.
Gilbert SF. Developmental Biology. 6th edition. Sunderland (MA): Sinauer Associates; 2000. Available from: https://www.ncbi.nlm.nih.gov/books/NBK9983/
Gobbi, G., and Janiri, L. (2006). Sodium- and magnesium-valproate in vivo modulate glutamatergic and GABAergic synapses in the medial prefrontal cortex. Psychopharmacology (Berl) 185, 255-262.
Göttlicher M, Minucci S, Zhu P, Krämer OH, Schimpf A, Giavara S, Sleeman JP, Lo Coco F, Nervi C, Pelicci PG, Heinzel T. Valproic acid defines a novel class of HDAC inhibitors inducing differentiation of transformed cells. EMBO J. 2001 Dec 17;20(24):6969-78. doi: 10.1093/emboj/20.24.6969. PMID: 11742974; PMCID: PMC125788.
Goyal R, Spencer KA, Borodinsky LN. From Neural Tube Formation Through the Differentiation of Spinal Cord Neurons: Ion Channels in Action During Neural Development. Front Mol Neurosci. 2020 Apr 24;13:62. doi: 10.3389/fnmol.2020.00062. PMID: 32390800; PMCID: PMC7193536.
Greene ND, Copp AJ. Development of the vertebrate central nervous system: formation of the neural tube. Prenat Diagn. 2009 Apr;29(4):303-11. doi: 10.1002/pd.2206. PMID: 19206138.
Greene ND & Copp, A. J. (2014). Neural tube defects. Annual review of neuroscience, 37, 221–242. https://doi.org/10.1146/annurev-neuro-062012-170354
Gu X, Spitzer NC. Distinct aspects of neuronal differentiation encoded by frequency of spontaneous Ca2+ transients. Nature. 1995 Jun 29;375(6534):784-7. doi: 10.1038/375784a0. PMID: 7596410.

Gurvich, N., Berman, M.G., Wittner, B.S., Gentleman, R.C., Klein, P.S., and Green, J.B. (2005). Association of valproate-induced teratogenesis with histone deacetylase inhibition in vivo. FASEB J 19, 1166-1168.

Hanson MG, Landmesser LT. Characterization of the circuits that generate spontaneous episodes of activity in the early embryonic mouse spinal cord. J Neurosci. 2003 Jan 15;23(2):587-600. doi: 10.1523/JNEUROSCI.23-02-00587.2003. PMID: 12533619; PMCID: PMC6741864.

Harden CL. Antiepileptic drug teratogenesis: what are the risks for congenital malformations and adverse cognitive outcomes? Int Rev Neurobiol. 2008;83:205-13. doi: 10.1016/S0074-7742(08)00011-1. PMID: 18929083.

Harden CL, Hopp J, Ting TY, Pennell PB, French JA, Allen Hauser W, Wiebe S, Gronseth GS, Thurman D, Meador KJ, Koppel BS, Kaplan PW, Robinson JN, Gidal B, Hovinga CA, Wilner AN, Vazquez B, Holmes L, Krumholz A, Finnell R, Le Guen C; American Academy of Neurology; American Epilepsy Society. Management issues for women with epilepsy-Focus on pregnancy (an evidence-based review): I. Obstetrical complications and change in seizure frequency: Report of the Quality Standards Subcommittee and Therapeutics and Technology Assessment Subcommittee of the American Academy of Neurology and the American Epilepsy Society. Epilepsia. 2009 May;50(5):1229-36. doi: 10.1111/j.1528-1167.2009.02128.x. PMID: 19496807.

Harland R. Neural induction. Curr Opin Genet Dev. 2000 Aug;10(4):357-62. doi: 10.1016/s0959-437x(00)00096-4. PMID: 10889069.

Harris, M.J., and Juriloff, D.M. (2010). An update to the list of mouse mutants with neural tube closure defects and advances toward a complete genetic perspective of neural tube closure. Birth Defects Res A Clin Mol Teratol 88, 653-669.

Hiilesmaa VK. Pregnancy and birth in women with epilepsy. Neurology. 1992 Apr;42(4 Suppl 5):8-11. PMID: 1574182.

Hill DS, Wlodarczyk BJ, Palacios AM, Finnell RH. Teratogenic effects of antiepileptic drugs. Expert Rev Neurother 2010;10:943–959.

Holmes LB, Harvey EA, Coull BA, Huntington KB, Khoshbin S, Hayes AM and Ryan LM: The teratogenicity of anticonvulsant drugs. N Engl J Med. 344:1132–1138. 2001.

Hull JM, Isom LL. Voltage-gated sodium channel β subunits: The power outside the pore in brain development and disease. Neuropharmacology. 2018 Apr;132:43-57. doi: 10.1016/j.neuropharm.2017.09.018. Epub 2017 Sep 18. PMID: 28927993; PMCID: PMC5856584.

Humphries AC, Narang S, Mlodzik M. Mutations associated with human neural tube defects display disrupted planar cell polarity in Drosophila. Elife. 2020 Apr 1;9:e53532. doi: 10.7554/eLife.53532. PMID: 32234212; PMCID: PMC7180057.

Ikonomidou C, Turski L. Antiepileptic drugs and brain development. Epilepsy Res 2010;88:11–22.

Kallen, A.J. (1994). Maternal carbamazepine and infant spina bifida. Reprod Toxicol 8, 203-205.

Kaneko, S., Battino, D., Andermann, E., Wada, K., Kan, R., Takeda, A., Nakane, Y., Ogawa, Y., Avanzini, G., Fumarola, C., et al. (1999). Congenital malformations due to antiepileptic drugs. Epilepsy Res 33, 145-158.

Kapur RP, Hoyle GW, Mercer EH, Brinster RL, Palmiter RD. Some neuronal cell populations express human dopamine beta-hydroxylase-lacZ transgenes transiently during embryonic

development. Neuron. 1991 Nov;7(5):717-27. doi: 10.1016/0896-6273(91)90275-5. PMID: 1742022.
Keller, R., Shih, J., and Domingo, C. (1992a). The patterning and functioning of protrusive activity during convergence and extension of the Xenopus organiser. Dev Suppl, 81-91.
Keller, R., Shih, J., and Sater, A. (1992b). The cellular basis of the convergence and extension of the Xenopus neural plate. Developmental dynamics: an official publication of the American Association of Anatomists193, 199-217.
Keller, R., Shih, J., Sater, A.K., and Moreno, C. (1992c). Planar induction of convergence and extension of the neural plate by the organizer of Xenopus. Developmental dynamics : an official publication of the American Association of Anatomists193, 218-234.
Keller-Peck, C.R., and Mullen, R.J. (1997). Altered cell proliferation in the spinal cord of mouse neural tube mutants curly tail and Pax3 splotch-delayed. Brain research. Developmental brain research 102, 177-188.
Kellogg M, Meador KJ. Neurodevelopmental Effects of Antiepileptic Drugs. Neurochem Res. 2017 Jul;42(7):2065-2070. doi: 10.1007/s11064-017-2262-4. Epub 2017 Apr 19. PMID: 28424947; PMCID: PMC6390972.
Kelly, T.E. (1984a). Teratogenicity of anticonvulsant drugs. I: Review of the literature. Am J Med Genet 19, 413-434.
Kelly, T.E., Rein, M., and Edwards, P. (1984b). Teratogenicity of anticonvulsant drugs. IV: The association of clefting and epilepsy. Am J Med Genet 19, 451-458.
Khokha, M. K., Chung, C., Bustamante, E. L., Gaw, L. W., Trott, K. A., Yeh, J., Grammer, T. C. (2002). Techniques and probes for the study of Xenopus tropicalis development. Dev Dyn, 225(4), 499-510. doi:10.1002/dvdy.10184
Ko, G.Y., Brown-Croyts, L.M., and Teyler, T.J. (1997). The effects of anticonvulsant drugs on NMDA-EPSP, AMPA-EPSP, and GABA-IPSP in the rat hippocampus. Brain Res Bull 42, 297-302.
Kuo CC, Chen RS, Lu L, Chen RC. Carbamazepine inhibition of neuronal Na+ currents: quantitative distinction from phenytoin and possible therapeutic implications. Mol Pharmacol. 1997 Jun;51(6):1077-83. doi: 10.1124/mol.51.6.1077. PMID: 9187275.
Kuo CC. A common anticonvulsant binding site for phenytoin, carbamazepine, and lamotrigine in neuronal Na+ channels. Mol Pharmacol. 1998 Oct;54(4):712-21. PMID: 9765515.
Laeng, P., Pitts, R.L., Lemire, A.L., Drabik, C.E., Weiner, A., Tang, H., Thyagarajan, R., Mallon, B.S., and Altar, C.A. (2004). The mood stabilizer valproic acid stimulates GABA neurogenesis from rat forebrain stem cells. Journal of neurochemistry 91, 238-251.
Lauder, J.M., Wallace, J.A., and Krebs, H. (1981). Roles for serotonin in neuroembryogenesis. Adv Exp Med Biol 133, 477-506.
Leach MJ, Marden CM, Miller AA. Pharmacological studies on lamotrigine, a novel potential antiepileptic drug: II. Neurochemical studies on the mechanism of action. Epilepsia. 1986;27(5):490–497.
Lee CH & Ruben PC (2008) Interaction between voltage-gated sodium channels and the neurotoxin, tetrodotoxin, Channels, 2:6, 407-412, DOI: 10.4161/chan.2.6.7429
Lindhout D, Hoppener RJ, Meinardi H. Teratogenicity of antiepileptic drug combinations with special emphasis on epoxidation (of carbamazepine) Epilepsia. 1984;25(1):77–83
Little, B.B., Santos-Ramos, R., Newell, J.F., and Maberry, M.C. (1993). Megadose carbamazepine during the period of neural tube closure. Obstet Gynecol 82, 705-708.

Loscher, W., 2002. Basic pharmacology of valproate: a review after 35 years of clinical use for the treatment of epilepsy. CNS Drugs 16 (10), 669–694.
LoTurco, J.J., Owens, D.F., Heath, M.J., Davis, M.B., and Kriegstein, A.R. (1995). GABA and glutamate depolarize cortical progenitor cells and inhibit DNA synthesis. Neuron 15, 1287-1298.
Macdonald, R.L., Kelly, K.M., 1995. Antiepileptic drug mechanisms of action. Epilepsia 36(Suppl. 2), S2–S12.
Marek KW, Kurtz LM, Spitzer NC. cJun integrates calcium activity and tlx3 expression to regulate neurotransmitter specification. Nat Neurosci. 2010; 13:944–950. PubMed: 20581840
Martin LJ, Corry B (2014) Locating the Route of Entry and Binding Sites of Benzocaine and Phenytoin in a Bacterial Voltage Gated Sodium Channel. PLOS Comput Biol 10(7): e1003688. doi:10.1371/journal.pcbi.1003688
Martin, E.D., and Pozo, M.A. (2004). Valproate reduced excitatory postsynaptic currents in hippocampal CA1 pyramidal neurons. Neuropharmacology 46, 555-561.
Martin ML, Regan CM. The anticonvulsant valproate teratogen restricts the glial cell cycle at a defined point in the mid-G1 phase. Brain Res. 1991 Jul 19;554(1-2):223-8. doi: 10.1016/0006-8993(91)90193-y. PMID: 1933304.
Messenger EA, Warner AE. The function of the sodium pump during differentiation of amphibian embryonic neurones. J Physiol. 1979 Jul;292:85-105. doi: 10.1113/jphysiol.1979.sp012840. PMID: 490420; PMCID: PMC1280847.
Moreau M, Néant I, Webb SE, Miller AL, Leclerc C. Calcium signalling during neural induction in Xenopus laevis embryos. Philos Trans R Soc Lond B Biol Sci. 2008 Apr 12;363(1495):1371-5. doi: 10.1098/rstb.2007.2254. PMID: 18198153; PMCID: PMC2610125.
Moretti ME, Bar-Oz B, Fried S, Koren G. Maternal hyperthermia and the risk for neural tube defects in offspring: systematic review and metaanalysis. Epidemiology. 2005;16:216–19.
Morimoto M, Satomura S, Hashimoto T, Kyotani S. A study of oxidative stress and the newer antiepileptic drugs in epilepsy associated with severe motor and intellectual disabilities. J Chin Med Assoc. 2017 Jan;80(1):19-28. doi: 10.1016/j.jcma.2016.10.005. Epub 2016 Nov 23. PMID: 27889457.
Nayak TK, Chakraborty S, Zheng W, Auerbach A. Structural correlates of affinity in fetal versus adult endplate nicotinic receptors. Nat Commun. 2016 Apr 22;7:11352. doi: 10.1038/ncomms11352. PMID: 27101778; PMCID: PMC4845029.
Nie, Q., Su, B., & Wei, J. (2016). Neurological teratogenic effects of antiepileptic drugs during pregnancy (Review). Experimental and Therapeutic Medicine, 12, 2400-2404. https://doi.org/10.3892/etm.2016.3628
Nieuwkoop, P. D., & Faber, J. (1994). Normal table of Xenopus laevis (Daudin) : a systematical and chronological survey of the development from the fertilized egg till the end of metamorphosis. New York: Garland Pub.
Nikolopoulou, E., Galea, G. L., Rolo, A., Greene, N. D., & Copp, A. J. (2017). Neural tube closure: cellular, molecular and biomechanical mechanisms. Development (Cambridge, England), 144(4), 552–566. https://doi.org/10.1242/dev.145904

O'Donovan MJ, Chub N, Wenner P. Mechanisms of spontaneous activity in developing spinal networks. J Neurobiol. 1998 Oct;37(1):131-45. doi: 10.1002/(sici)1097-4695(199810)37:1<131::aid-neu10>3.0.co;2-h. PMID: 9777737.

O'Leary ME, Chahine M. Mechanisms of Drug Binding to Voltage-Gated Sodium Channels. Handb Exp Pharmacol. 2018;246:209-231. doi: 10.1007/164_2017_73. PMID: 29138928.

Ohman I, Vitols S, Tomson T. Lamotrigine in pregnancy: pharmacokinetics during delivery, in the neonate, and during lactation. Epilepsia. 2000 Jun;41(6):709-13. doi: 10.1111/j.1528-1157.2000.tb00232.x. PMID: 10840403.

Ornoy A: Valproic acid in pregnancy: how much are we endangering the embryo and fetus? Reprod Toxicol. 28:1–10. 2009

Pai VP, Lemire JM, Paré JF, Lin G, Chen Y, Levin M. Endogenous gradients of resting potential instructively pattern embryonic neural tissue via Notch signaling and regulation of proliferation. J Neurosci. 2015 Mar 11;35(10):4366-85. doi: 10.1523/JNEUROSCI.1877-14.2015. PMID: 25762681; PMCID: PMC4355204.

Patsalos PN, Spencer EP, Berry DJ. Therapeutic Drug Monitoring of Antiepileptic Drugs in Epilepsy: A 2018 Update. Ther Drug Monit. 2018 Oct;40(5):526-548. doi: 10.1097/FTD.0000000000000546. PMID: 29957667.

Patterson, E.S., Waller, L.E., and Kroll, K.L. (2014). Geminin loss causes neural tube defects through disrupted progenitor specification and neuronal differentiation. Dev Biol 393, 44-56.

Perathoner S, Daane JM, Henrion U, Seebohm G, Higdon CW, Johnson SL, Nusslein-Volhard C, Harris MP. Bioelectric signaling regulates size in zebrafish fins. PLoS genetics. 2014;10:e1004080.

Phiel CJ, Zhang F, Huang EY, Guenther MG, Lazar MA, Klein PS. Histone deacetylase is a direct target of valproic acid, a potent anticonvulsant, mood stabilizer, and teratogen. J Biol Chem. 2001 Sep 28;276(39):36734-41. doi: 10.1074/jbc.M101287200. Epub 2001 Jul 25. PMID: 11473107.

Philbert A, Dam M. The epileptic mother and her child. Epilepsia. 1982 Feb;23(1):85-99. doi: 10.1111/j.1528-1157.1982.tb05055.x. PMID: 6799286.

Pippenger CE. Pharmacology of neural tube defects. Epilepsia. 2003;44 Suppl 3:24-32. doi: 10.1046/j.1528-1157.44.s3.3.x. PMID: 12790883.

Plazas PV, Nicol X, Spitzer NC. Activity-dependent competition regulates motor neuron axon pathfinding via PlexinA3. Proc Natl Acad Sci U S A. 2013; 110:1524–1529. [PubMed: 23302694]

Ramlochansingh, C., Branoner, F., Chagnaud, B. P., & Straka, H. (2014). Efficacy of tricaine methanesulfonate (MS-222) as an anesthetic agent for blocking sensory-motor responses in Xenopus laevis tadpoles. PloS one, 9(7), e101606.

Ren J, Greer JJ. Ontogeny of rhythmic motor patterns generated in the embryonic rat spinal cord. Journal of neurophysiology. 2003; 89:1187–1195. [PubMed: 12626606]

Robinson KR, Stump RF. Self-generated electrical currents through Xenopus neurulae. J Physiol. 1984 Jul;352:339-52. doi: 10.1113/jphysiol.1984.sp015295. PMID: 6747892; PMCID: PMC1193215.

Rogawski, M.A., and Loscher, W. (2004). The neurobiology of antiepileptic drugs. Nat Rev Neurosci 5, 553-564.

Rogawski MA, Löscher W, Rho JM. Mechanisms of Action of Antiseizure Drugs and the Ketogenic Diet. Cold Spring Harb Perspect Med. 2016;6(5):a022780. Published 2016 May 2. doi:10.1101/cshperspect.a022780

Root, C.M., Velazquez-Ulloa, N.A., Monsalve, G.C., Minakova, E., and Spitzer, N.C. (2008). Embryonically expressed GABA and glutamate drive electrical activity regulating neurotransmitter specification. J Neurosci 28, 4777-4784.

Rosa, F.W. (1991). Spina bifida in infants of women treated with carbamazepine during pregnancy. N Engl J Med 324, 674-677.

Rowe SJ, Messenger NJ, Warner AE. The role of noradrenaline in the differentiation of amphibian embryonic neurons. Development. 1993 Dec;119(4):1343-57. doi: 10.1242/dev.119.4.1343. PMID: 8306892.

Sankaraneni R, Lachhwani D. Antiepileptic drugs--a review. Pediatr Ann. 2015 Feb;44(2):e36-42. doi: 10.3928/00904481-20150203-10. PMID: 25658217.

Schwarz, J.R., Grigat, G., 1989 May-Jun. Phenytoin and carbamazepine: potential- and frequency-dependent block of Na currents in mammalian myelinated nerve fibers. Epilepsia 30 (3), 286–294.

Sernagor E, Chub N, Ritter A, O'Donovan MJ. Pharmacological characterization of the rhythmic synaptic drive onto lumbosacral motoneurons in the chick embryo spinal cord. The Journal of neuroscience : the official journal of the Society for Neuroscience. 1995; 15:7452–7464. [PubMed: 7472497]

Session, A. M., Uno, Y., Kwon, T., Chapman, J. A., Toyoda, A., Takahashi, S., et al. (2016). Genome evolution in the allotetraploid frog Xenopus laevis. Nature 538, 336–343. doi: 10.1038/nature19840

Sequerra, E.B., Goyal, R., Castro, P.A., Levin, J.B., and Borodinsky, L.N. (2018). NMDA Receptor Signaling Is Important for Neural Tube Formation and for Preventing Antiepileptic Drug-Induced Neural Tube Defects. J Neurosci 38, 4762-4773.

Sills GJ, Rogawski MA. Mechanisms of action of currently used antiseizure drugs. Neuropharmacology. 2020 May 15;168:107966. doi: 10.1016/j.neuropharm.2020.107966. Epub 2020 Jan 14. PMID: 32120063.

Smith R. S., Walsh C. A. (2020). Ion channel functions in early brain development. Trends Neurosci. 43, 103–114. 10.1016/j.tins.2019.12.004

Spencer K. A., Belgacem Y. H., Visina O., Shim S., Genus H., Borodinsky L. N. (2019). Growth at cold temperature increases the number of motor neurons to optimize locomotor function. Curr. Biol. 29, 1787.e5–1799.e5. 10.1016/j.cub.2019.04.072

Spitzer, N. C., and Baccaglini, P. I. (1976). Development of the action potential in embryo amphibian neurons in vivo. Brain Res. 107, 610–616. doi: 10.1016/0006-8993(76)9014877

Spitzer NC, Gu X, Olson E. Action potentials, calcium transients and the control of differentiation of excitable cells. Curr Opin Neurobiol. 1994 Feb;4(1):70-7. doi: 10.1016/0959-4388(94)90034-5. PMID: 7513567.

Stefani A, Spadoni F, Siniscalchi A, Bernard G. Lamotrigine inhibits Calcium currents in cortical neurons: functional implications. Eur J Pharmacol. 1996;307:113–6.

Swapna, I., & Borodinsky, L. N. (2012). Interplay between electrical activity and bone morphogenetic protein signaling regulates spinal neuron differentiation. Proceedings of the National Academy of Sciences of the United States of America, 109(40), 16336–16341. https://doi.org/10.1073/pnas.1202818109

Tecoma ES. Oxcarbazepine. Epilepsia. 1999;40(Suppl 5):S37–S46.
Tennis P and Eldridge RR: International Lamotrigine Pregnancy Registry Scientific Advisory Committee: Preliminary results on pregnancy outcomes in women using lamotrigine. Epilepsia. 43:1161–1167. 2002.
Tu, M. K., & Borodinsky, L. N. (2014). Spontaneous calcium transients manifest in the regenerating muscle and are necessary for skeletal muscle replenishment. Cell calcium, 56(1), 34–41.
Urrego D, Tomczak AP, Zahed F, Stühmer W, Pardo LA. Potassium channels in cell cycle and cell proliferation. Philos Trans R Soc Lond B Biol Sci. 2014 Feb 3;369(1638):20130094. doi: 10.1098/rstb.2013.0094. PMID: 24493742; PMCID: PMC3917348.
Wallingford, J.B., Niswander, L.A., Shaw, G.M., and Finnell, R.H. (2013). The continuing challenge of understanding, preventing, and treating neural tube defects. Science 339, 1222002.
Warp E, Agarwal G, Wyart C, Friedmann D, Oldfield CS, Conner A, Del Bene F, Arrenberg AB, Baier H, Isacoff EY. Emergence of patterned activity in the developing zebrafish spinal cord. Current biology : CB. 2012; 22:93–102. [PubMed: 22197243]
Wegner, C., and Nau, H. (1992). Alteration of embryonic folate metabolism by valproic acid during organogenesis: implications for mechanism of teratogenesis. Neurology 42, 17-24.
Wlodarczyk, B. J., Palacios, A. M., George, T. M., & Finnell, R. H. (2012). Antiepileptic drugs and pregnancy outcomes. American journal of medical genetics. Part A, 158A(8), 2071–2090. https://doi.org/10.1002/ajmg.a.35438
Wu, C.F., Nakamura, H., Chan, A.P., Zhou, Y.H., Cao, T., Kuang, J., Gong, S.G., He, G., and Etkin, L.D. (2001). Tumorhead, a Xenopus gene product that inhibits neural differentiation through regulation of proliferation. Development 128, 3381-3393.
Yip TS, O'Doherty C, Tan NC, Dibbens LM, Suppiah V. SCN1A variations and response to multiple antiepileptic drugs. Pharmacogenomics J. 2014 Aug;14(4):385-9. doi: 10.1038/tpj.2013.43. Epub 2013 Dec 17. PMID: 24342961.
Zeise, M.L., Kasparow, S., and Zieglgansberger, W. (1991). Valproate suppresses N-methyl-D-aspartate evoked, transient depolarizations in the rat neocortex in vitro. Brain Res 544, 345-348.
Zheng, J.Q., and Poo, M.M. (2007). Calcium signaling in neuronal motility. Annu Rev Cell Dev Biol 23, 375-404.
Zona C, Tancredi V, Longone P, D'Arcanfelo G, D'Antuono M, Manfred M, et al. Neocortical potassium currents are enhanced by the antiepileptic drug lamotrigine. Epilepsia. 2002;43:685–90.